The Abdus Salam
International Centre for Theoretical Physics

United Nations
Educational, Scientific
and Cultural Organization

International Atomic
Energy Agency

SMR.1664 - 11

Conference on Single Molecule Magnets and Hybrid Magnetic Nanostructures

27 June - 1 July 2005

Bulk Transport Properties of Single Molecule Magnets and other interesting Materials

Naresh S. DALAL
Department of Chemistry & Biochemistry
Center for Magnetic Resonance
National High Magnetic Field Laboratory
Florida State University
Tallahassee, FL 32306-4390
U.S.A.

Bulk Transport Properties of Single Molecule Magnets and other Interesting Materials

Dr. Naresh Dalal

Collaborators

- Dr. David Zipse
- Dr. Micah North
- Professor James Brooks
- Professor Steve Hill
- Professor George Christou
- Professor Andrew Kent
- Professor Dave Hendrickson
- Professor Jan Musfeldt
- Dr. Paul Kögerler (Ames Laboratory)
- MARTECH
- NSF/NIRT (Grant No. DMR 0103290)

Transport Outline

- Motivation
- Background and Techniques
- Compounds and Discussion
  - SMM (Mn_{12}-Ac and Fe_8Br_8)
  - V_{12} and V_{15}
- Conclusions
- Future Work

Motivation

- Magnetic Semiconductors are rare
- Spintronics Applications
- Band Structure Characterization

Semiconductors

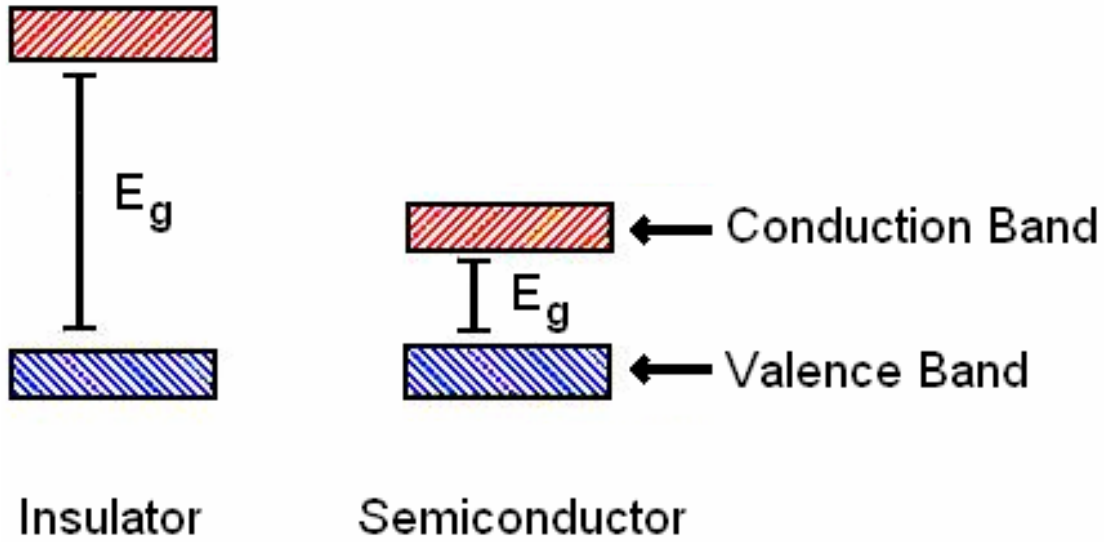

- $R(T) \approx \exp(E_a/k_B T)$
- Comprised of a filled valence band and an empty conduction band.
- C. Kittel, Solid State Physics:
  $E_a = \frac{1}{2}E_g + \frac{3}{4}k_b T \ln(m_h/m_e)$
- E_g represents the optical band gap
- E_a represents the transport band gap
- E_g for a semiconductor is typically around 1eV
- Assuming $m_h = m_e \rightarrow 2E_a \approx E_g$

Four Probe Technique for *dc* Resistivity

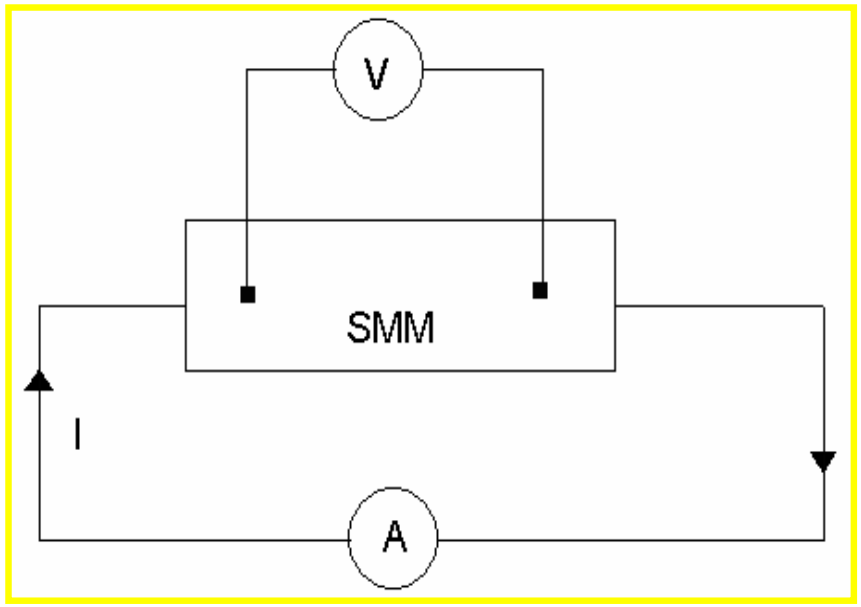

- Four probe technique for constant current measurements (FIMV)
- Two probe for constant voltage measurements (FVMI)
- Constant currents typically 0.1 nA – 10 nA
- Constant voltages typically ≈ 100 V

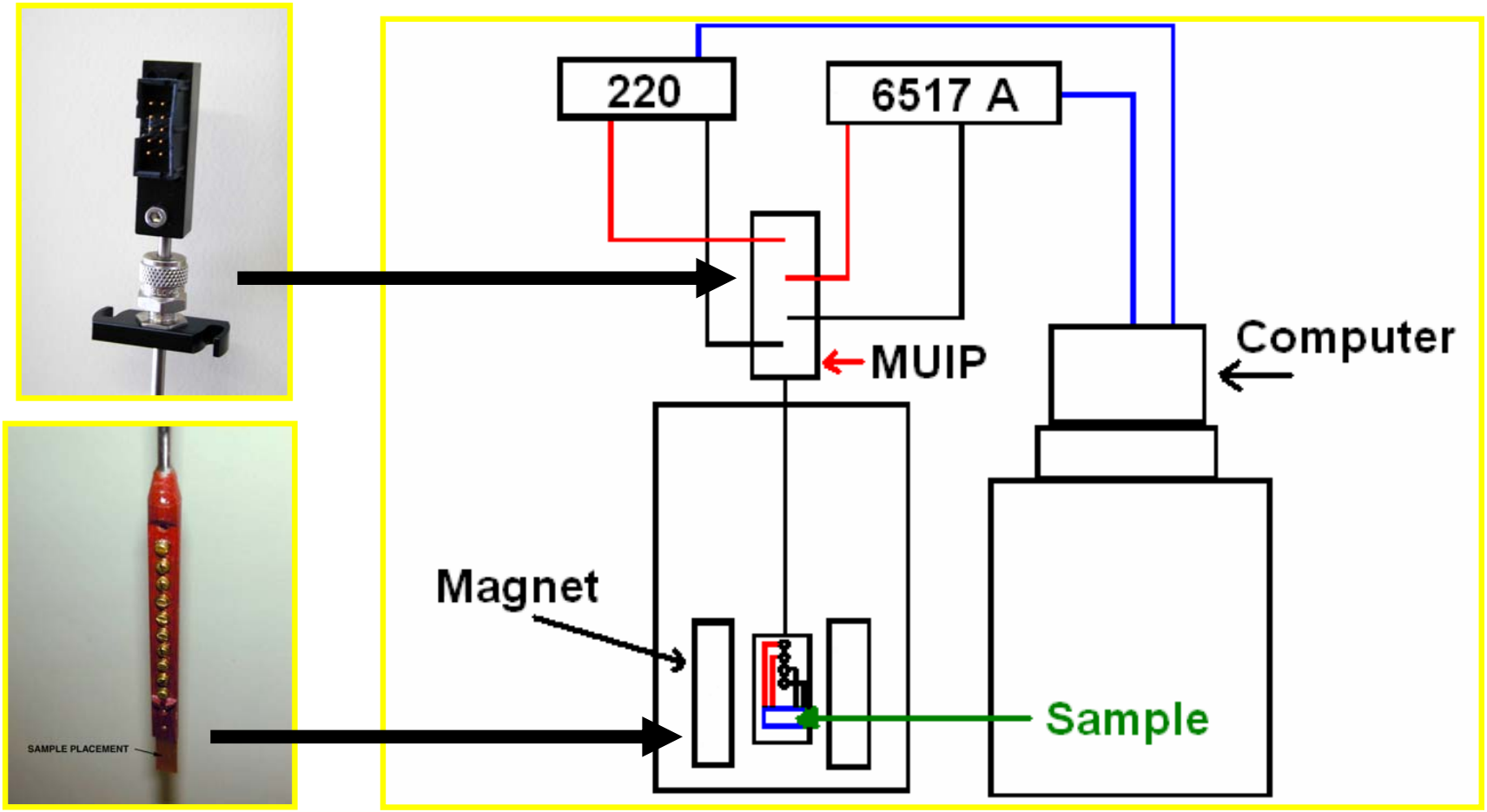

- Keithley 220 low level current source
- Keithley 6517A High resistivity electrometer
- SQUID gives precise temperature control, inert atmosphere, and the ability to apply magnetic fields

Semiconductive Behavior of Mn_{12} and Fe_8

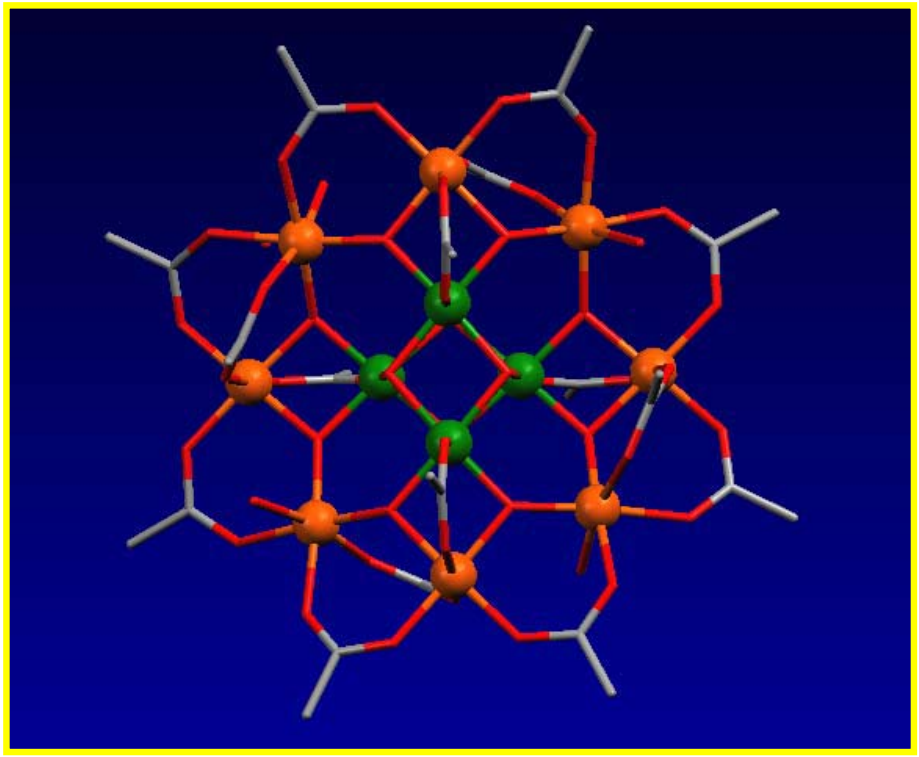

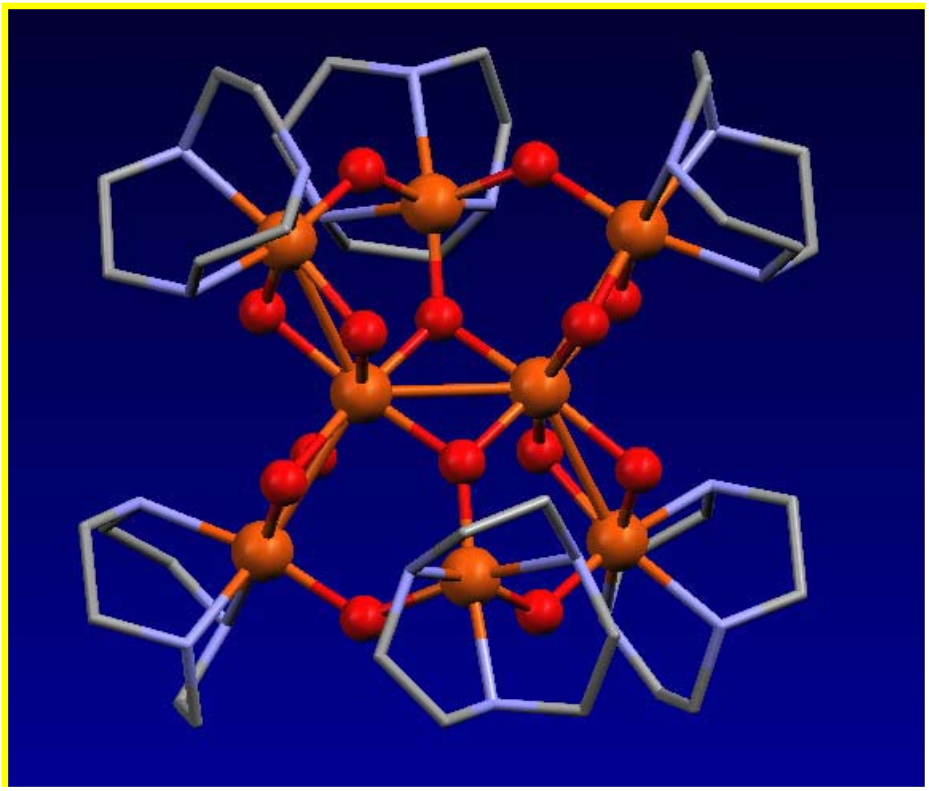

Mn_{12}-Ac

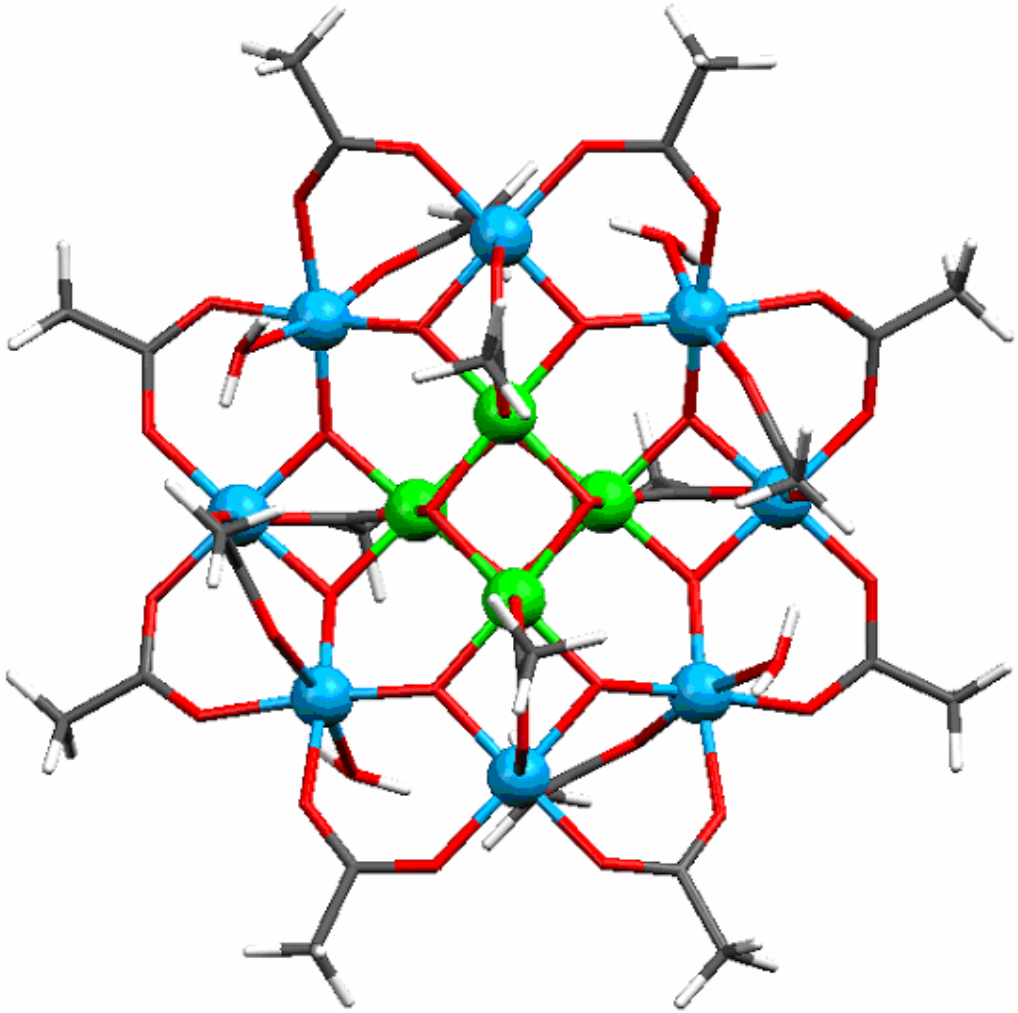

Mn^{3+}

Mn^{4+}

Oxygen

Carbon

Hydrogen

Dielectric Studies of Mn_{12}-ac

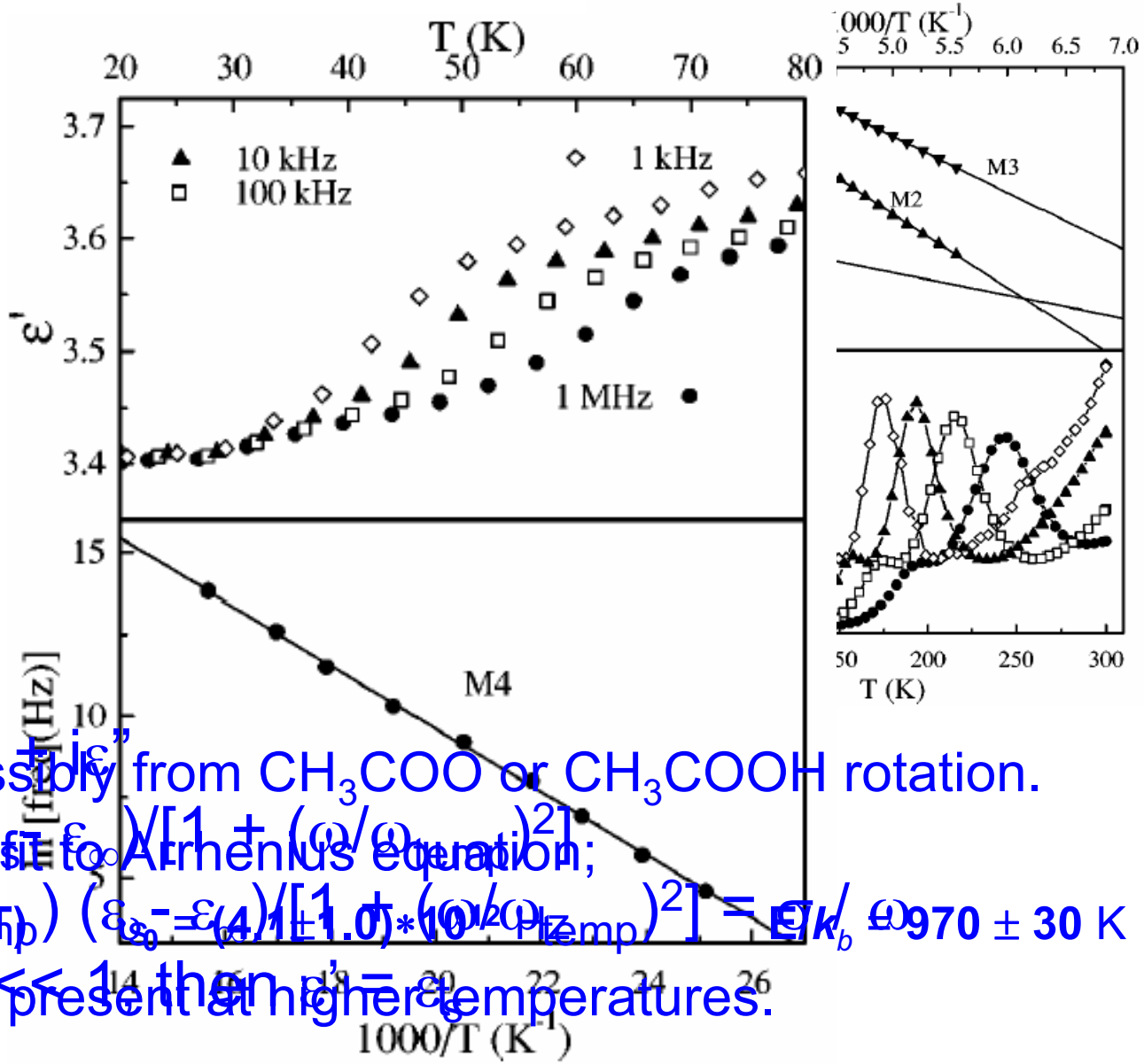

- Mode M4 possibly from CH_3COO or CH_3COOH rotation.
- M4 data was fit to Arrhenius equation;
- $\upsilon = \upsilon_0 \exp(-E/k_b T)$ $E/k_b = 970 \pm 30$ K
- Other Modes present at higher temperatures.

$\varepsilon(\omega, T) = \varepsilon' \pm j\varepsilon''$

$\varepsilon' = \varepsilon_\infty + (\varepsilon_s - \varepsilon_\infty)/[1 + (\omega/\omega_{relaxation})^2]$

$\varepsilon'' = (\omega/\omega_{relaxation}) (\varepsilon_s - \varepsilon_\infty)/[1 + (\omega/\omega_{relaxation})^2]$

If $(\omega/\omega_{relaxation}) << 1$ then $\varepsilon' = \varepsilon_s$

$\omega_{relaxation} = (4.1 \pm 1.0) * 10^{12} \exp(-E/k_b T_{temp})$

Mn_{12}-Acetate (constant current)

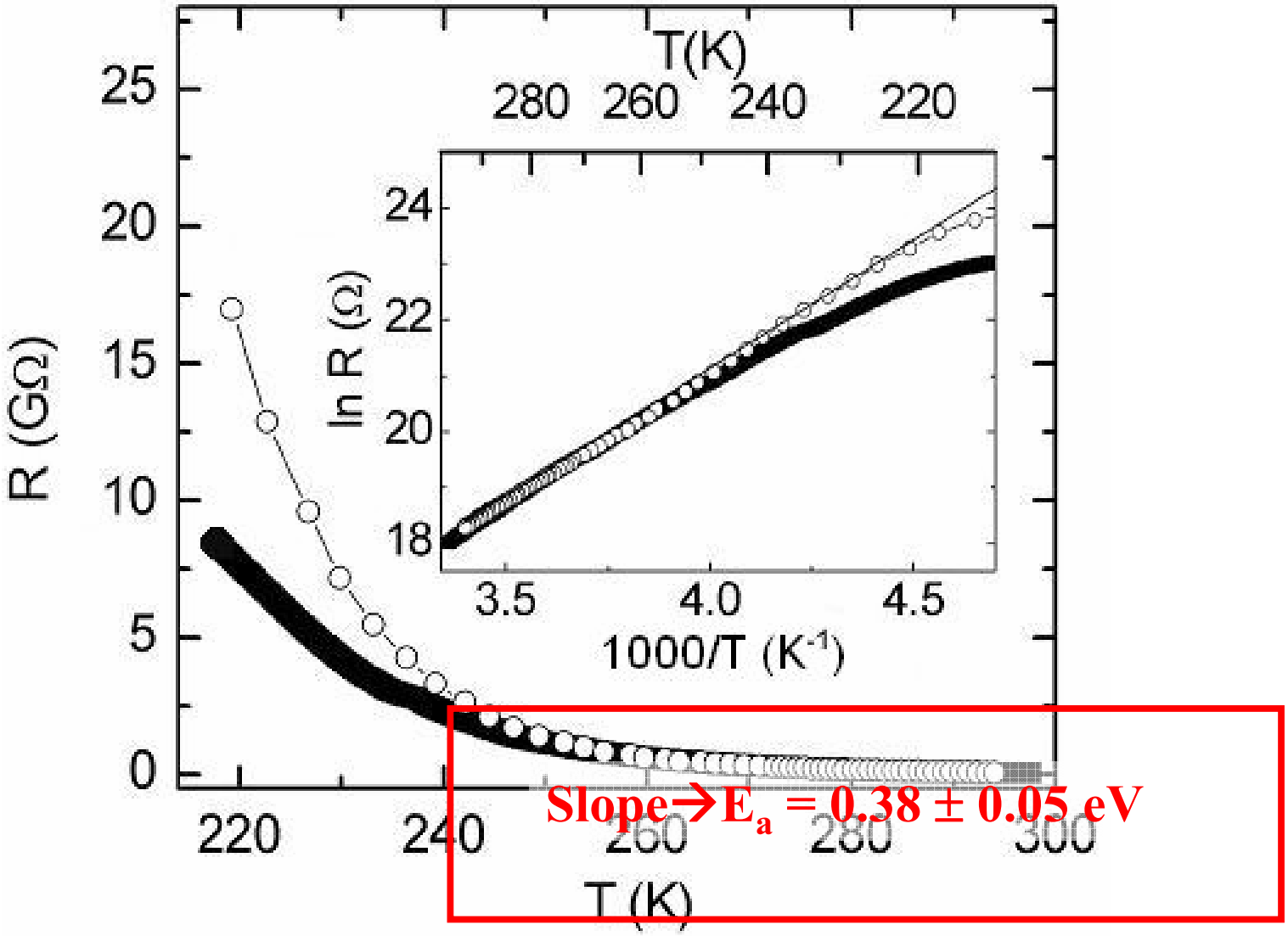

- Conductivity $\propto$ $DOS_{band\ edge}$ x exp $(-E_a/k_bT)$

Mn_{12}-Acetate (constant voltage)

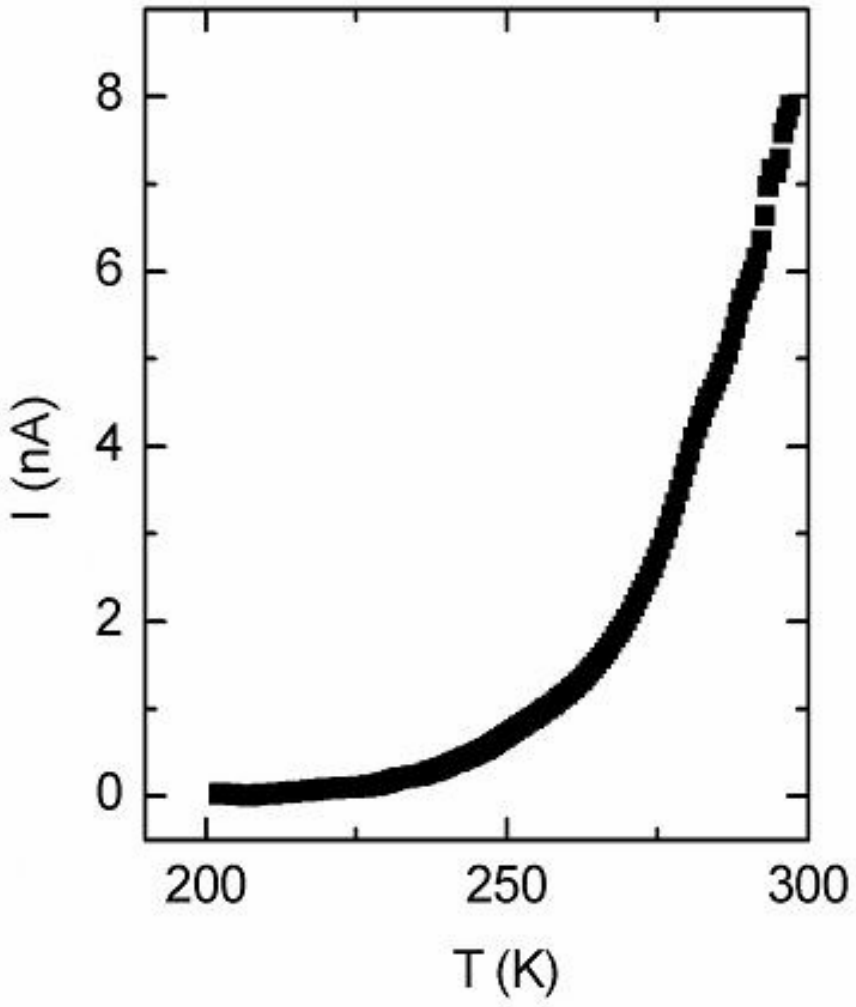

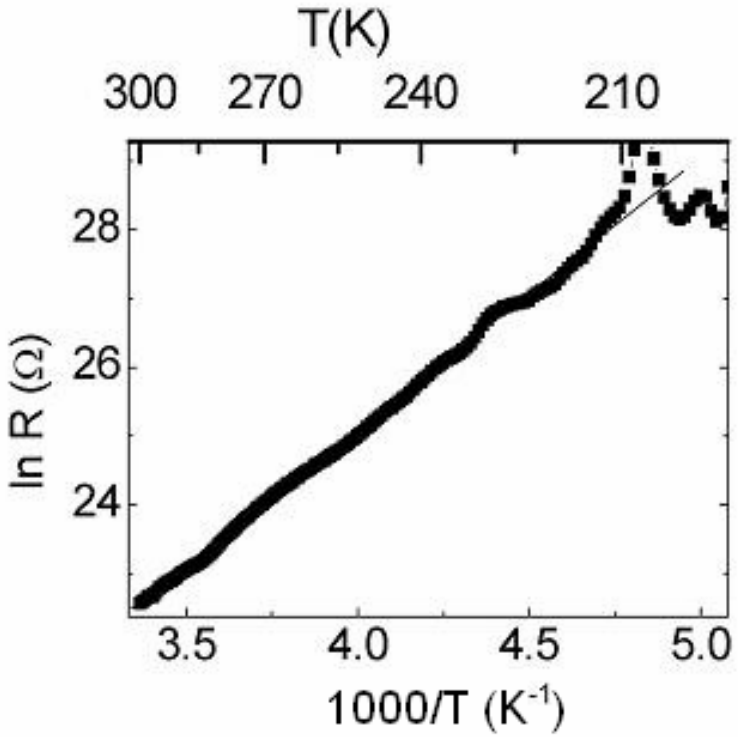

Slope→ $E_a = 0.36 \pm 0.05$ eV

North, *et al. Phys. Rev. B* **67,** 174407 (2003).

Possible Conduction Pathway for Mn_{12}-ac

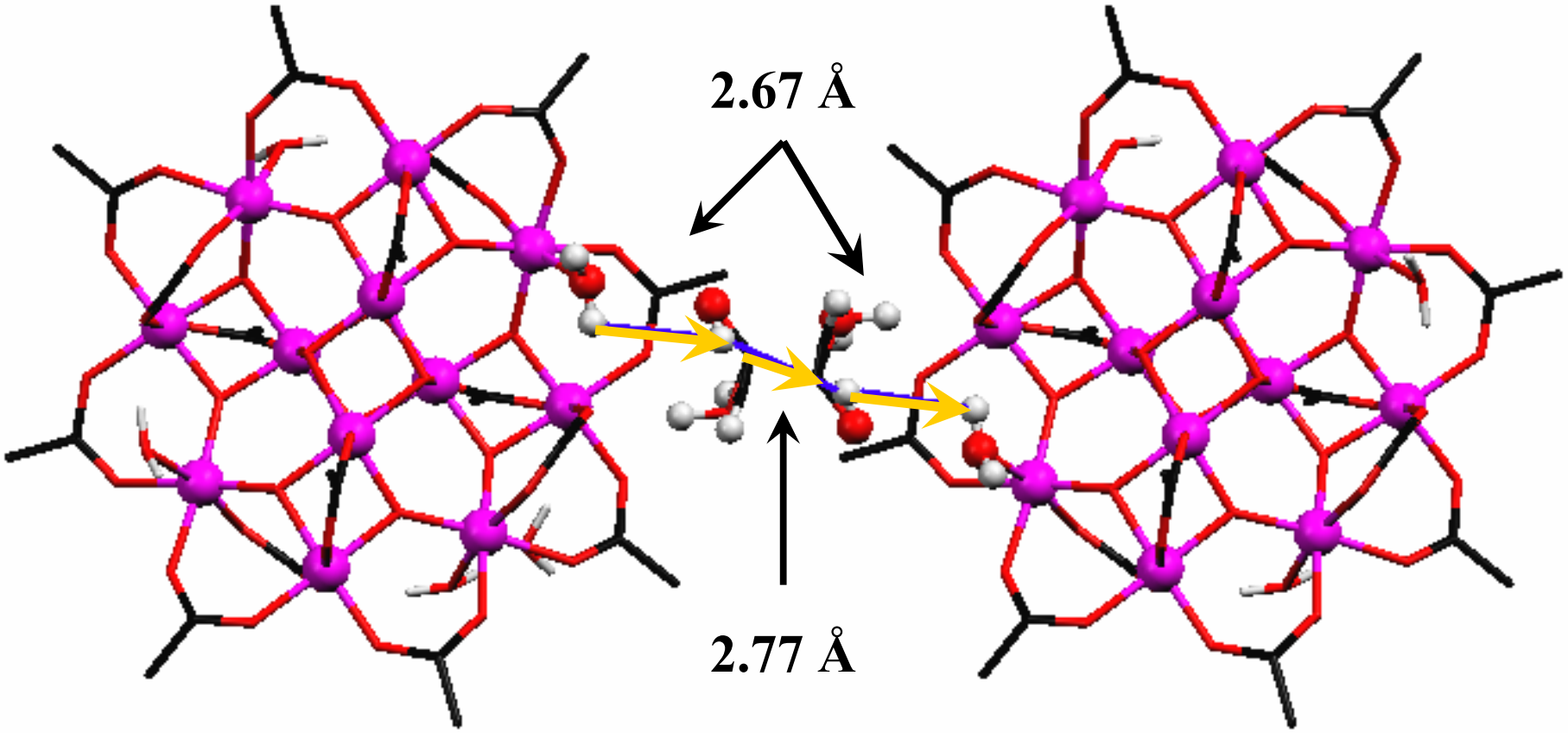

Mn-H_2O→acetate→acetate→H_2O-Mn

Photoconductivity of Mn_{12}-ac

- A factor of about eight increase in the photoconductivity is observed when going from 632.8 nm to 488 nm.
- Optical data show only a factor of two increase in absorption over this range.
- This rules out a direct heating effect.

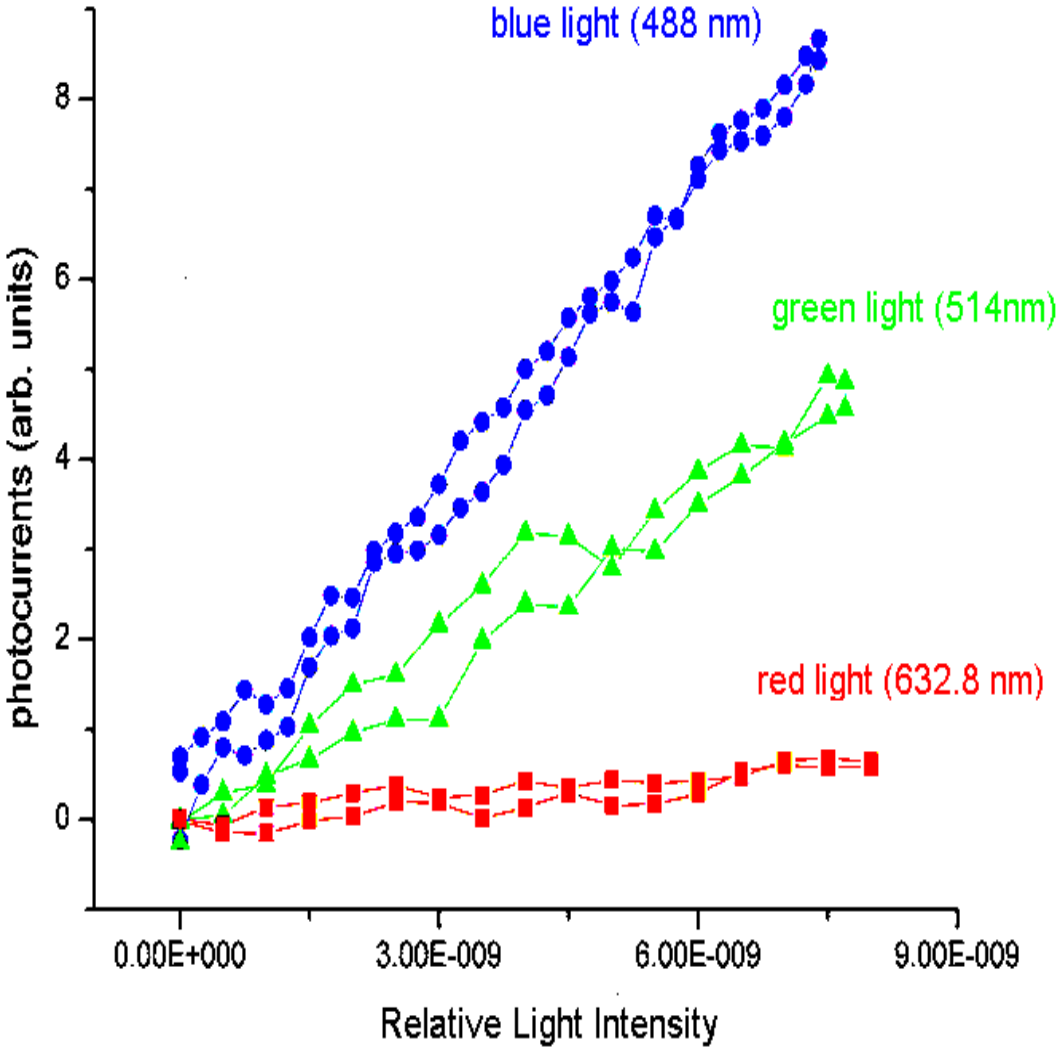

Fe_8Br_8

- **Fe^{3+} ($3d^5$): S=5/2**
- $6Fe^{3+}$ for S=15 ↑
- $2Fe^{3+}$ for S=5 ↓
- Total 15-5; S=10

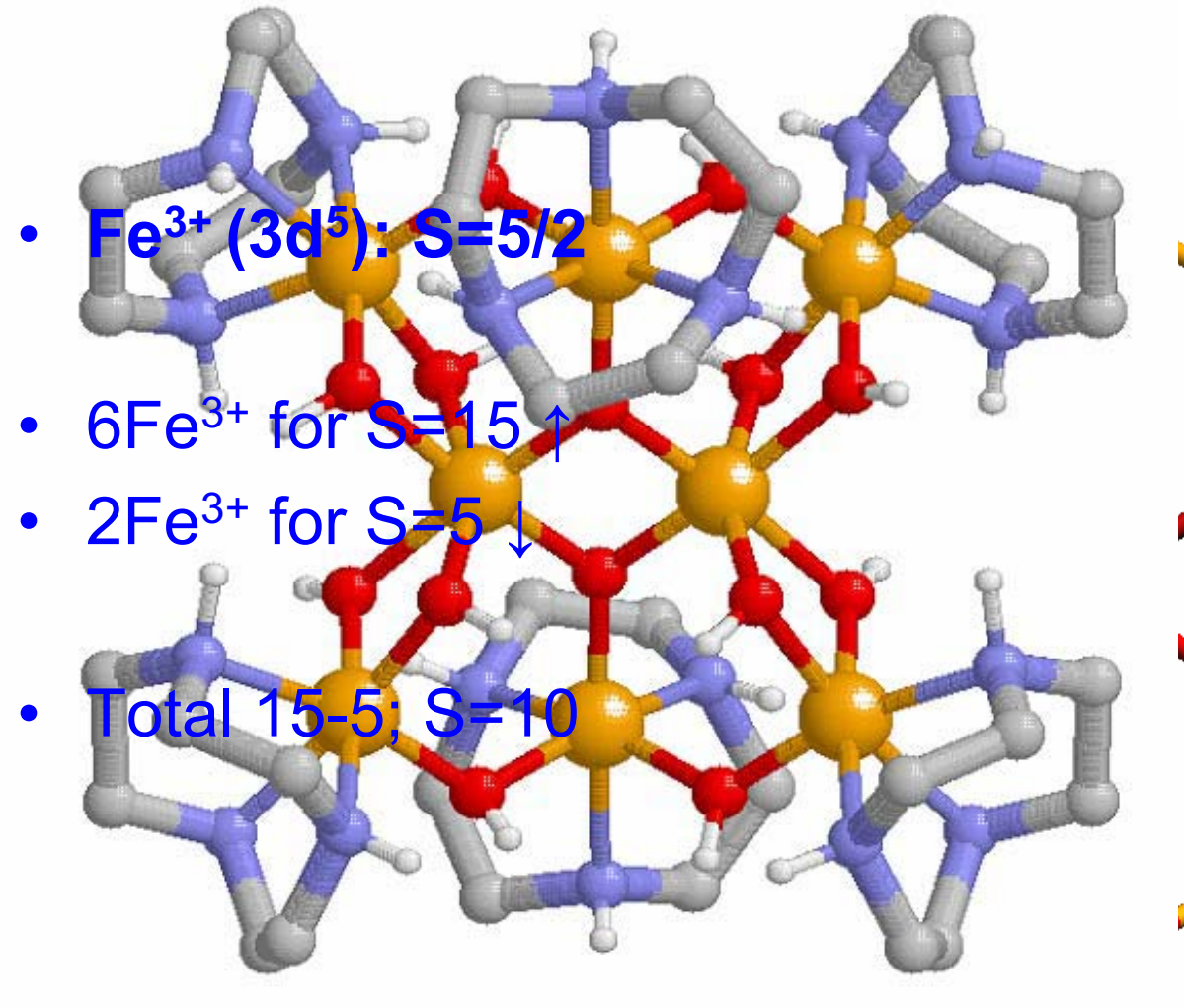

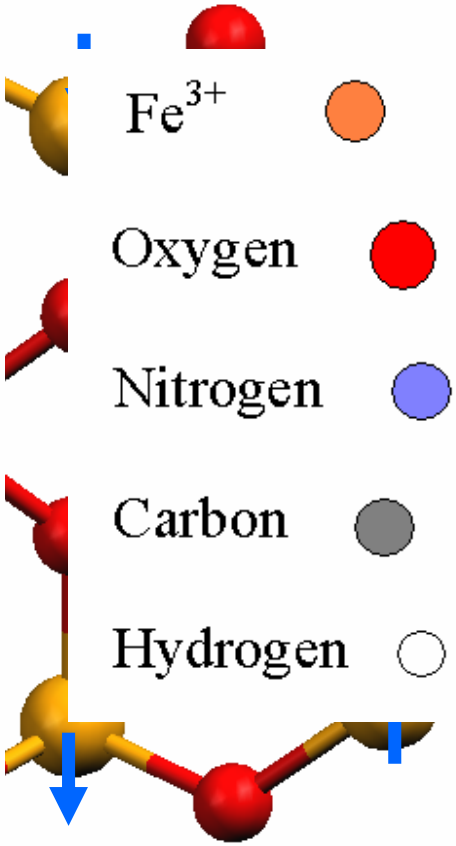

Resistivity of Fe_8

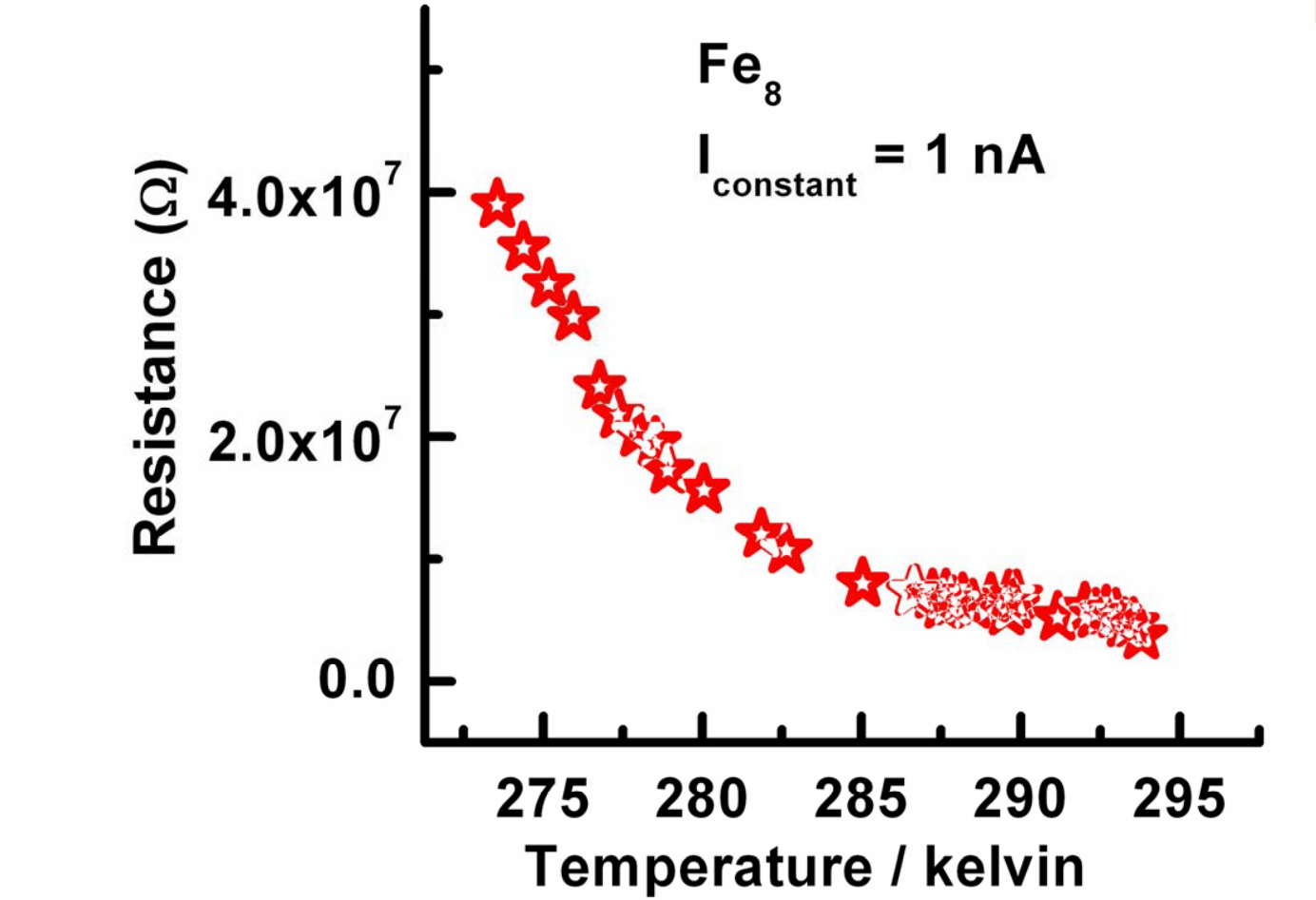

North, *et al. Phys. Rev. B* **67,** 174407 (2003).

Possible Conduction Pathway for Fe_8Br_8

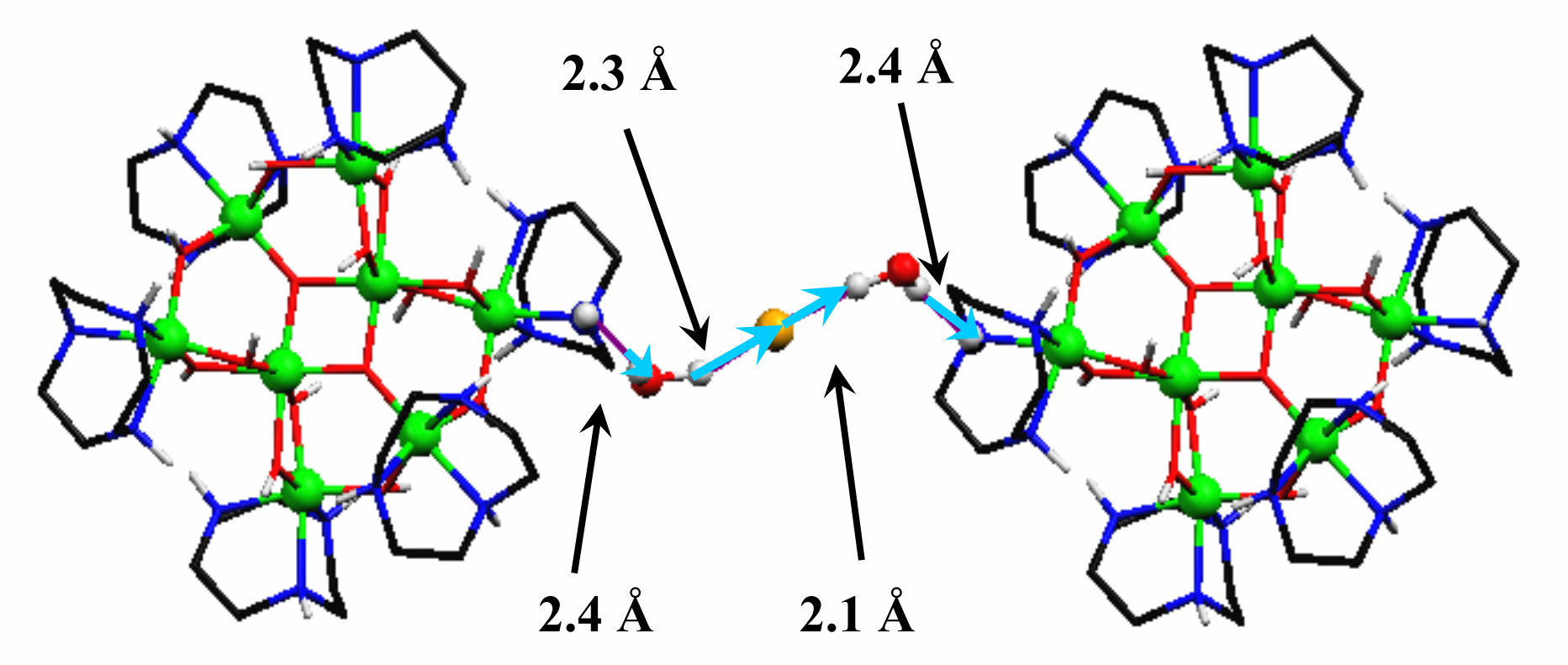

Fe-N-H→H_2O→Br^-→H_2O→H-N-Fe

SMM Conductivity Summary

- Mn_{12}-ac and Fe_8 show semiconductor behavior with band gaps of ~0.7 eV and ~1.5 eV respectively, both could be classified as intrinsic semiconductors because $E_a \approx \frac{1}{2} E_g$
- Mn_{12}-ac exhibits photoconductivity in visible region. Fe_8Br_8 to be checked.
- Proposed conduction pathways are consistent with the higher activation energy found in Fe_8Br_8.
- Density of States near band edges for both materials is quite small.

J. M. North *et al.*, *Phys. Rev. B* **67**, 174407-1-7 (2003).

Semiconductive Behavior of V_{12} and V_{15}

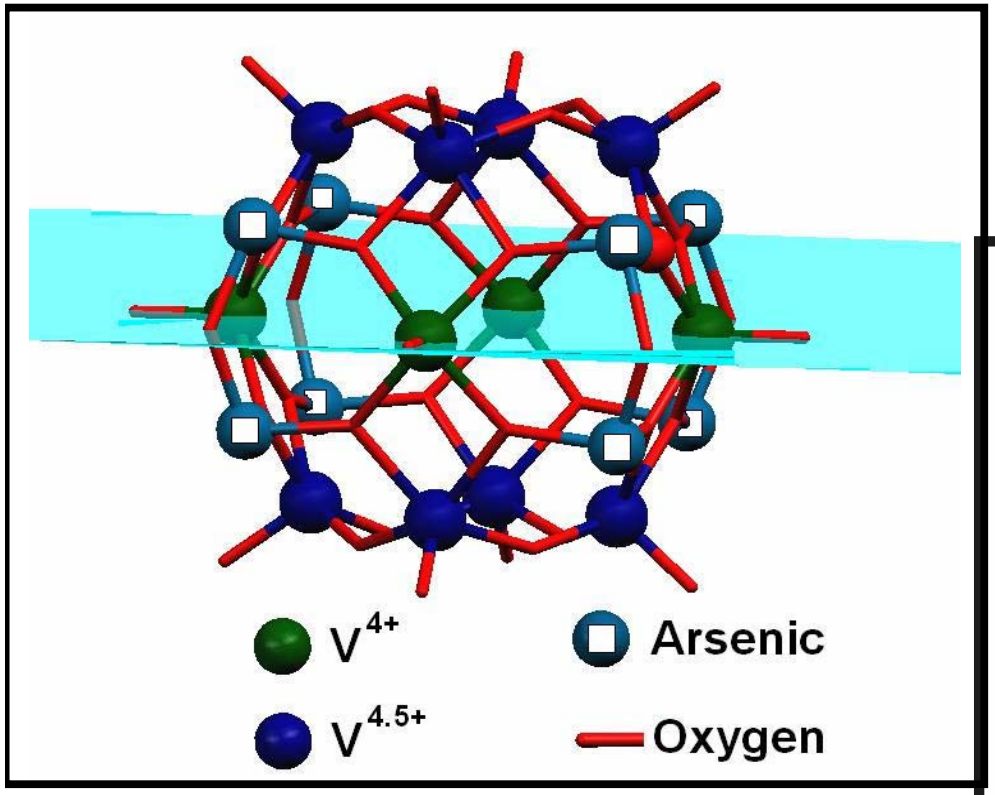

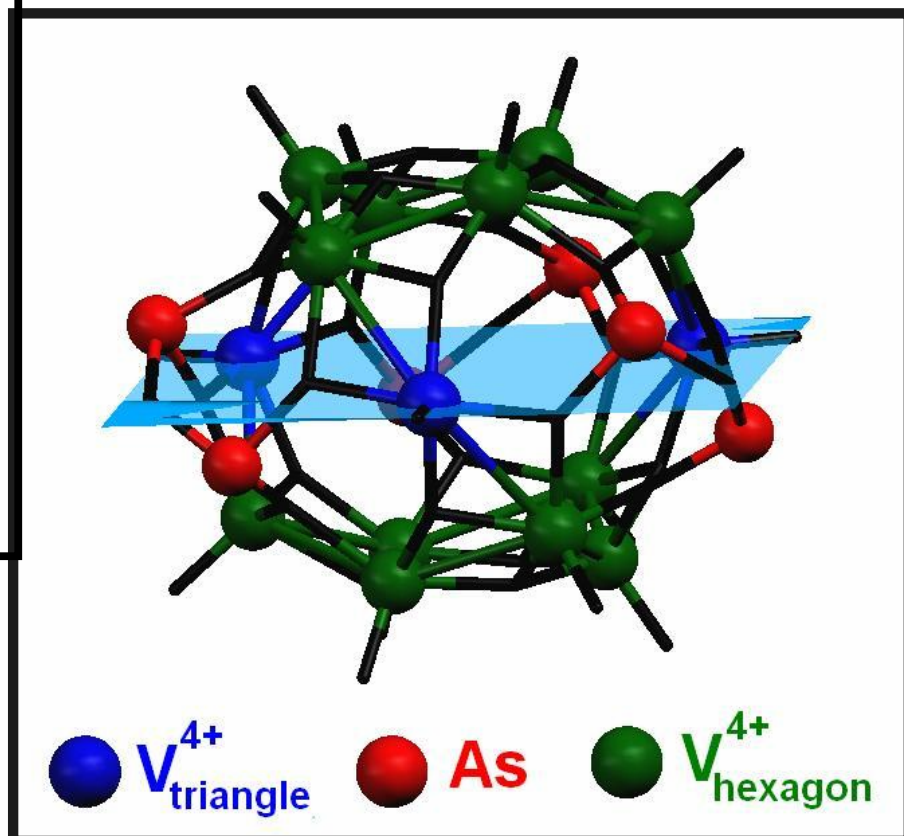

$[NH(C_2H_5)_3]_4[V_8^{4.5+}V_4^{4+}As_8O_{40}(H_2O)] \cdot H_2O$ (V_{12})

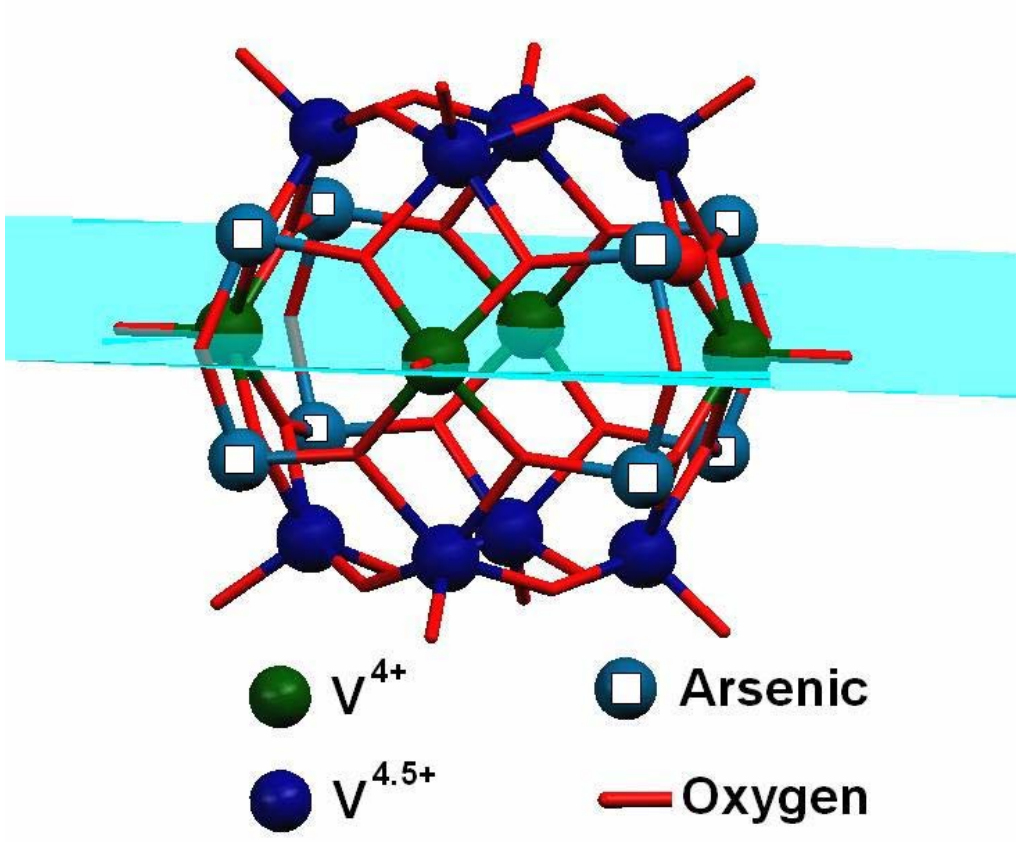

Pope *et al*. *Angew. Chem., Int. Ed. Engl.* **30**, 32 (1991).

- ***S* = 0**
- **Two d electrons delocalized amongst four vandiums in top and bottom layers**
- **Four V^{4+} ions in middle layer**
- **Weak antiferromagnetic interactions (≈18 K) between V^{4+} ions**

Resistivity of V_{12}

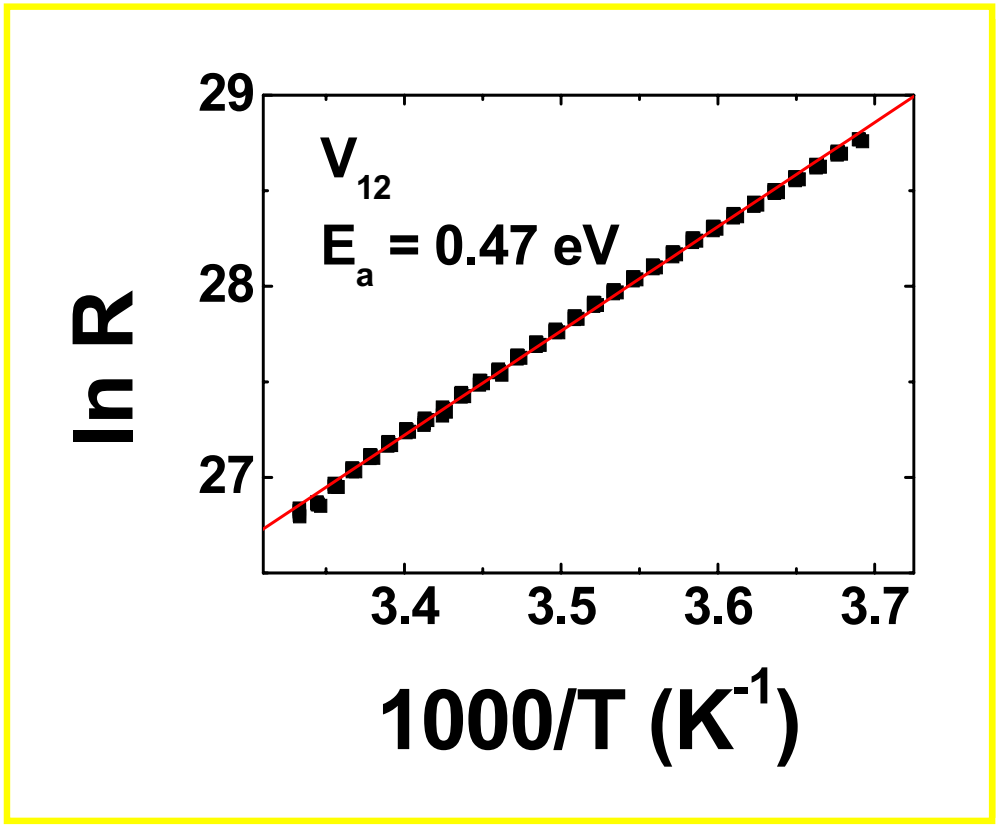

- Constant voltage configuration,
  V_{const} = 250 V
  T = 270 – 300 K
- Constant Current configuration,
  I_{const} = 200 pA
- E_a = 0.48 ± 0.05 eV

Optical Band Gap vs. Transport Gap for V_{12}

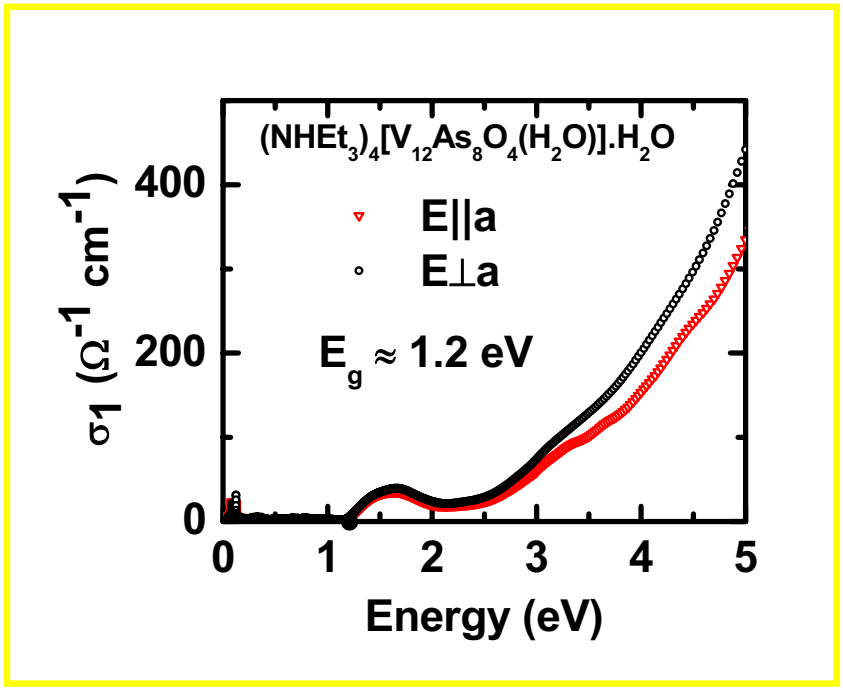

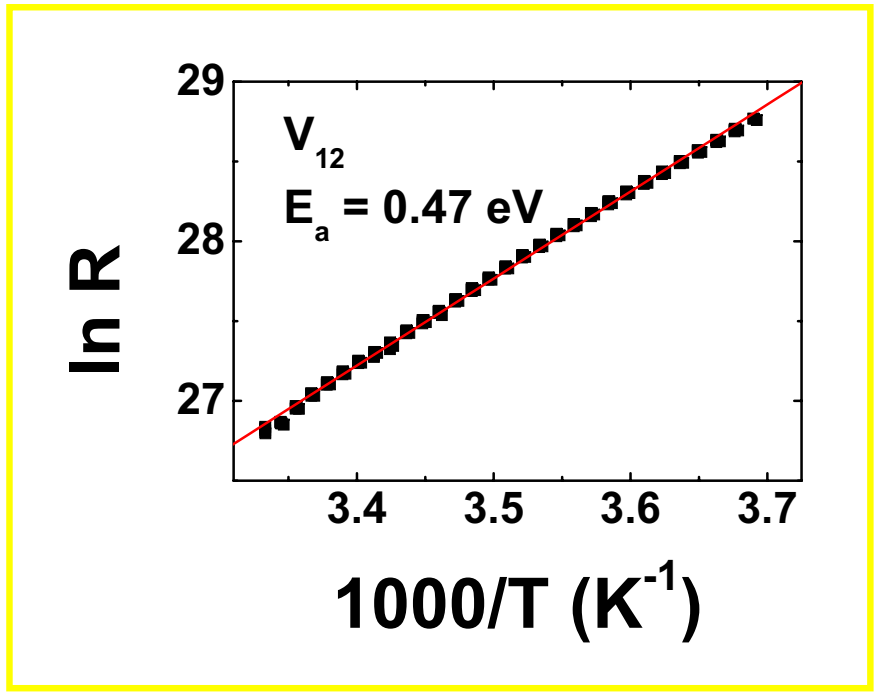

- In an intrinsic semiconductor $E_g \approx 2E_a$
- $E_g \approx 1.2$ eV ≈ 2 (0.48 eV)

$K_6[V_{15}As_6O_{42}(H_2O)] \cdot 8H_2O$

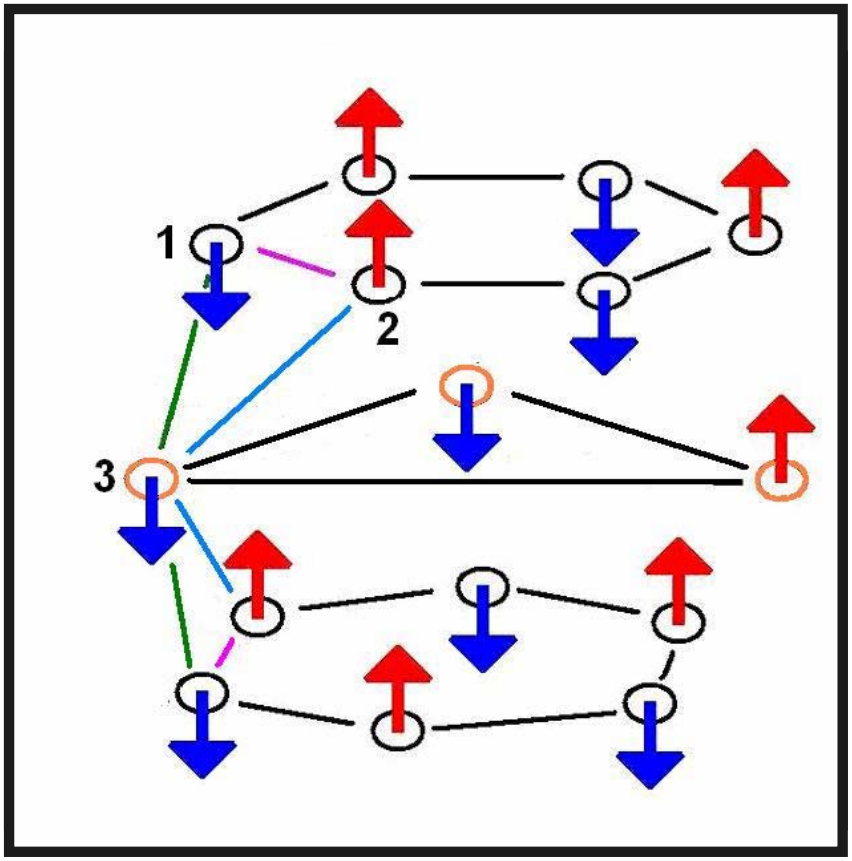

Müller *et al. Angew. Chem., Int. Ed. Engl.* **27,** 1721 (1988).

- 15 V^{4+} ions all antiferromagnetically coupled
- $J_{1\text{-}2} >> J_{2\text{-}3} > J_{1\text{-}3}$
- Equilateral triangle of *s* = ½ ions
- Ground state doublets split (0.05 K) by Dzyaloshinskii-Moriya interactions - QTM

Dielectric Relaxation of V_{15}

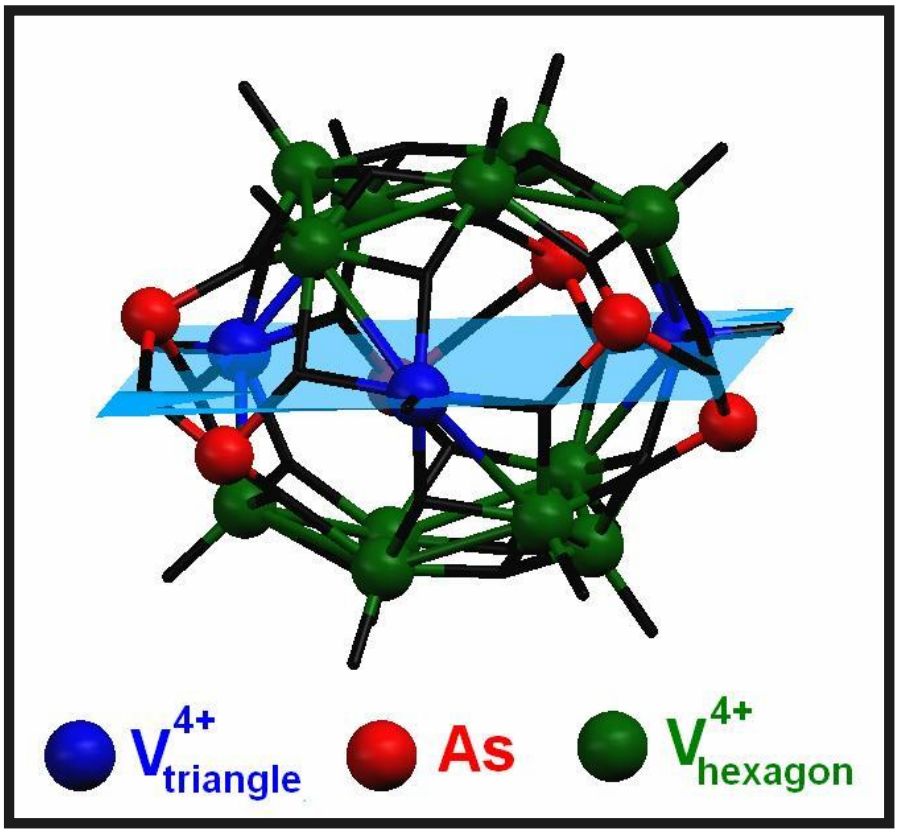

- Determine the dielectric constant for theoretical work
- Dielectric relaxation studies give insight into low frequency motional dynamics
- *Ac* impedance bridge technique (SR830 DSP Lock-in Amplifier)
- 77 – 330 K; 500 Hz – 250 kHz; 1 V drive amplitude

Dielectric Relaxation Modes

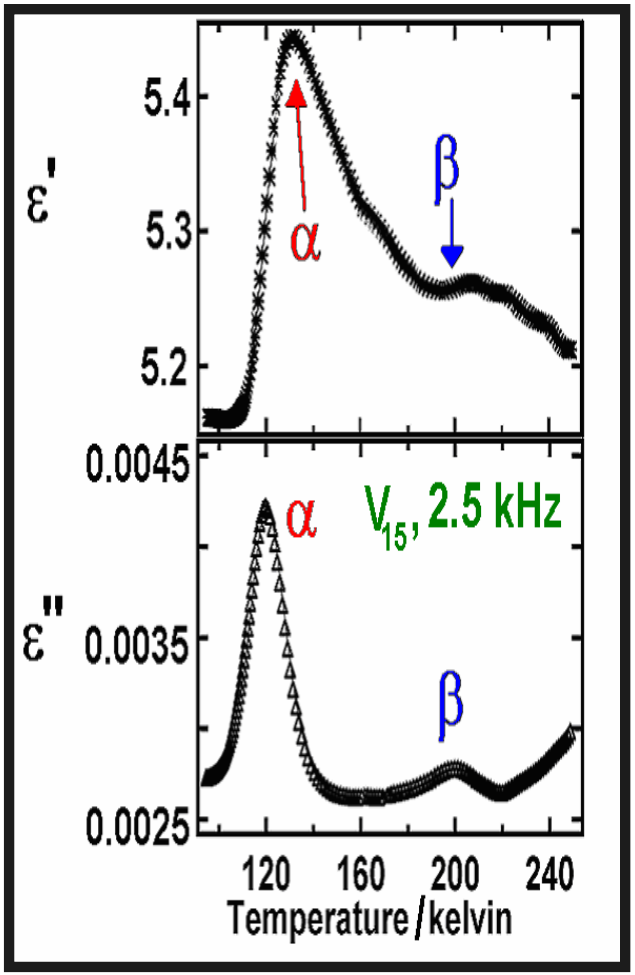

- $\varepsilon(\omega,T) = \varepsilon' + i\varepsilon''$
- $\varepsilon' = \varepsilon_\infty + (\varepsilon_s - \varepsilon_\infty)/[1 + (\omega/\omega_{temp})^2]$
- $\varepsilon'' = (\omega/\omega_{temp})\,(\varepsilon_s - \varepsilon_\infty)/[1 + (\omega/\omega_{temp})^2]$
  $= \sigma / \omega$
- If $(\omega/\omega_{temp}) << 1$, then $\varepsilon' = \varepsilon_s$
- $\varepsilon_s = (C \times d) / (A \times \varepsilon_0) = 6 \pm 1$
- α peak well fit by Gaussian function for all experimental frequencies
- ε_s relatively temperature independent

Temperature Dependence of α mode

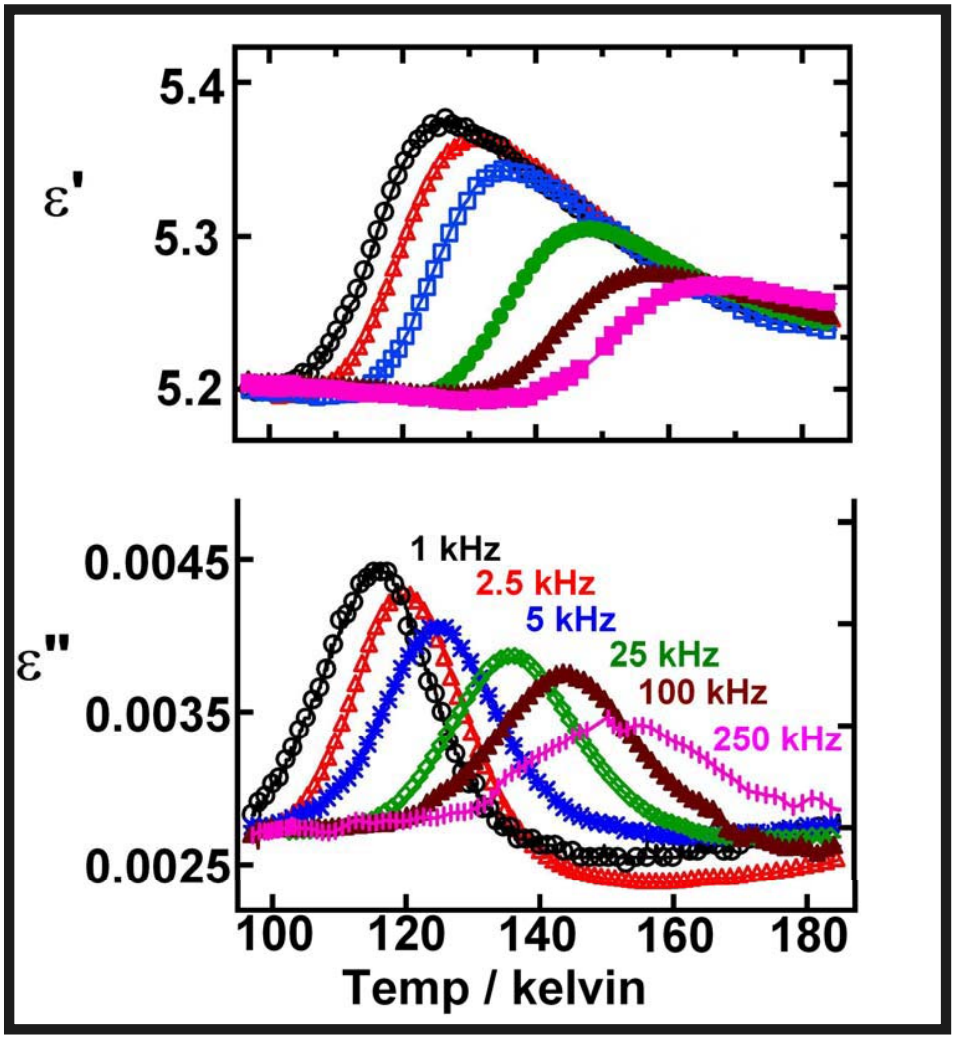

- Peak in ε" corresponds to $\omega = \omega_{temp}$
- Step-like decrease of ε' and ε" indicative of a slowing of the dielectric relaxation with decreasing temperature

Arrhenius Analysis

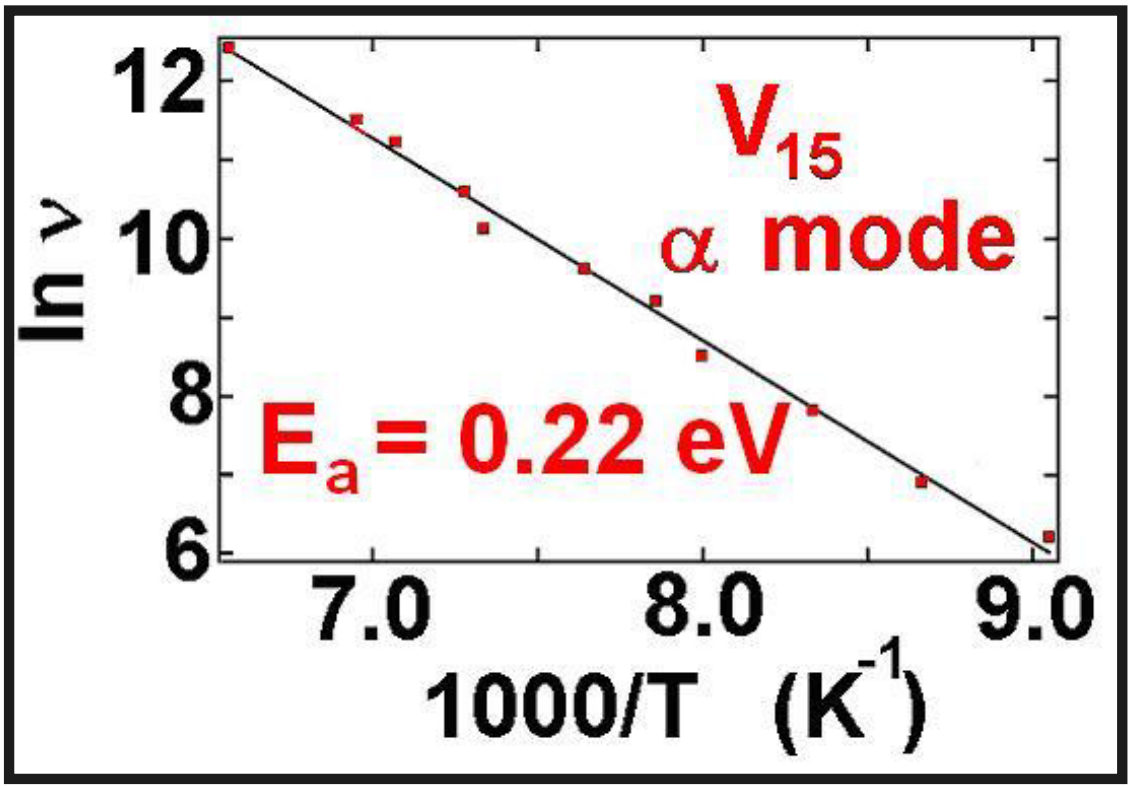

- Activation energy to dipole reorientation = 0.22 ± 0.05 eV
- $\nu_0 \approx 1 \times 10^{13}$ Hz (333 cm^{-1}) (vibrational mode)

Vibrational Modes of V_{15}

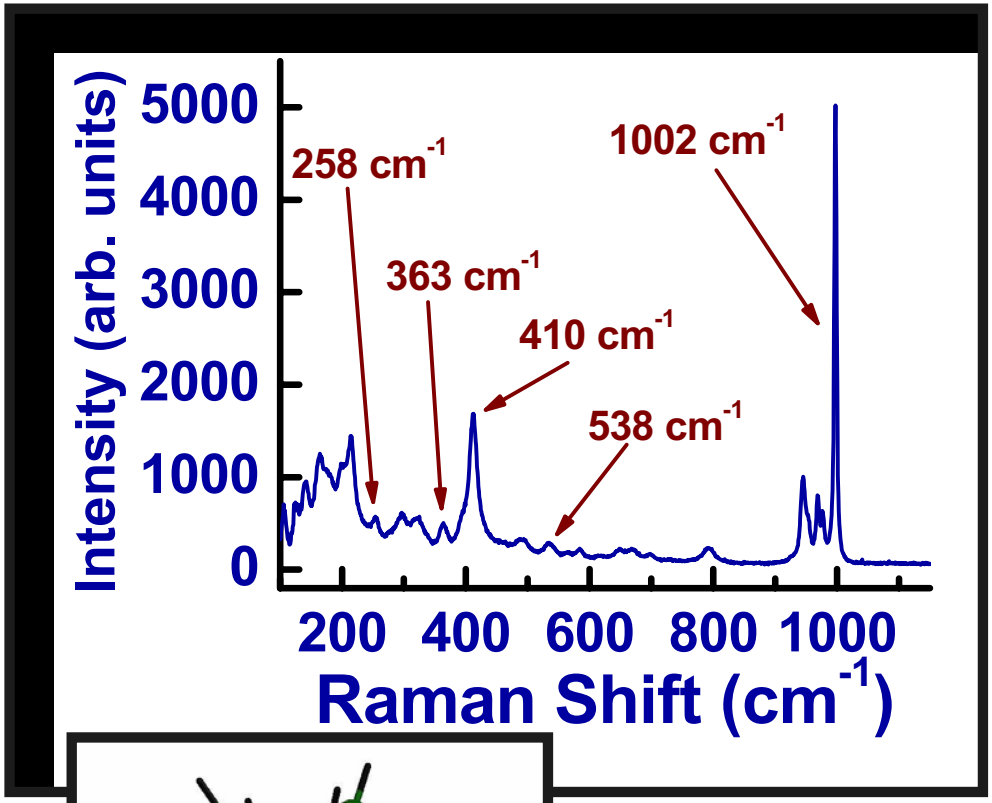

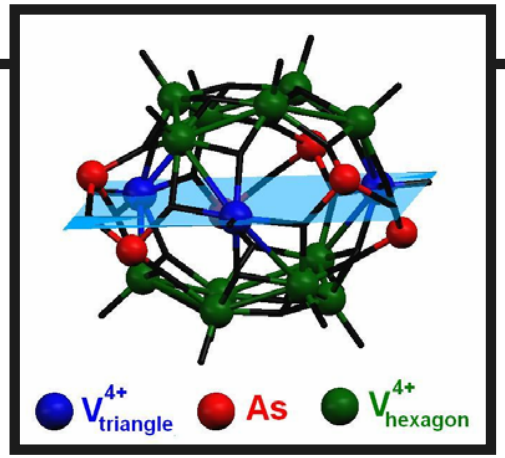

- 538 cm^{-1} – V – O internal stretch
- 410 cm^{-1} – O – V – O bend
- 363 cm^{-1} - As – O – As bend
- 258 cm^{-1} – O – As – O bend
- R (120 K) ~ 1 TΩ
- Vibrational modes provide mechanism for dipole reorientation

Induced Polarization

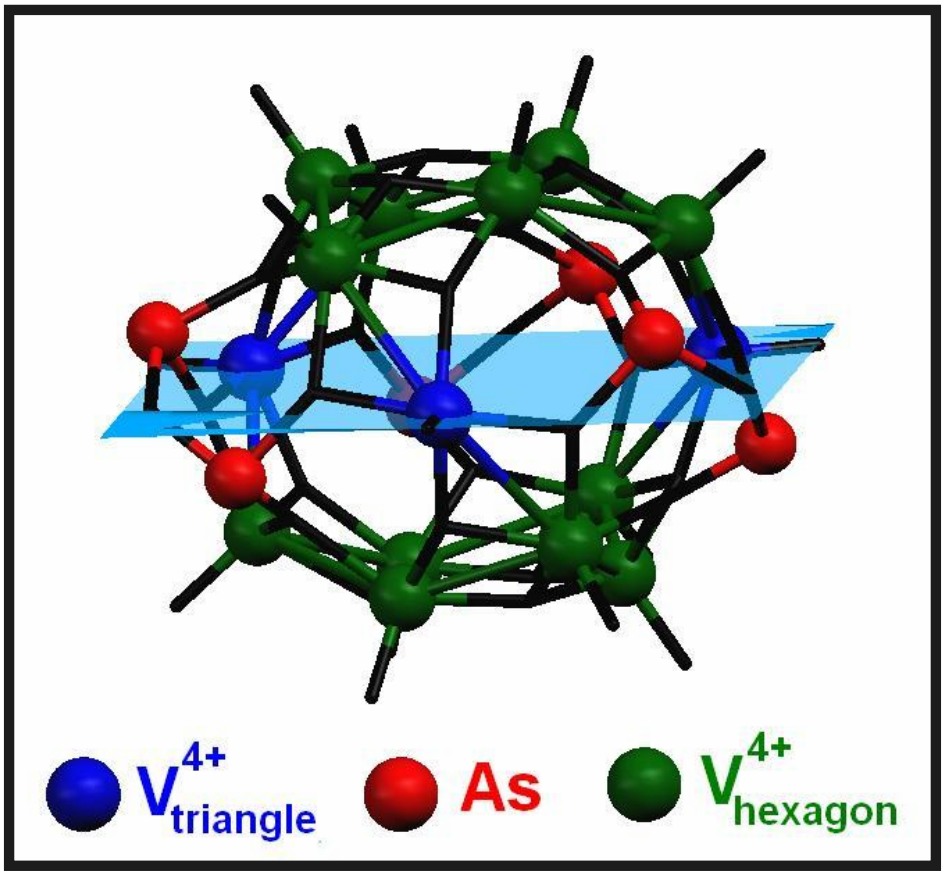

- ε_s has little or no temperature dependence
- $\varepsilon_s \propto (P + \mu^2/3k_BT)$
- No permanent dipole
- Vibrations responsible for dipole reorientation

Onsager, *J. Am. Chem. Soc.* **58**, 1486 (1936).

Resistivity of V_{15}

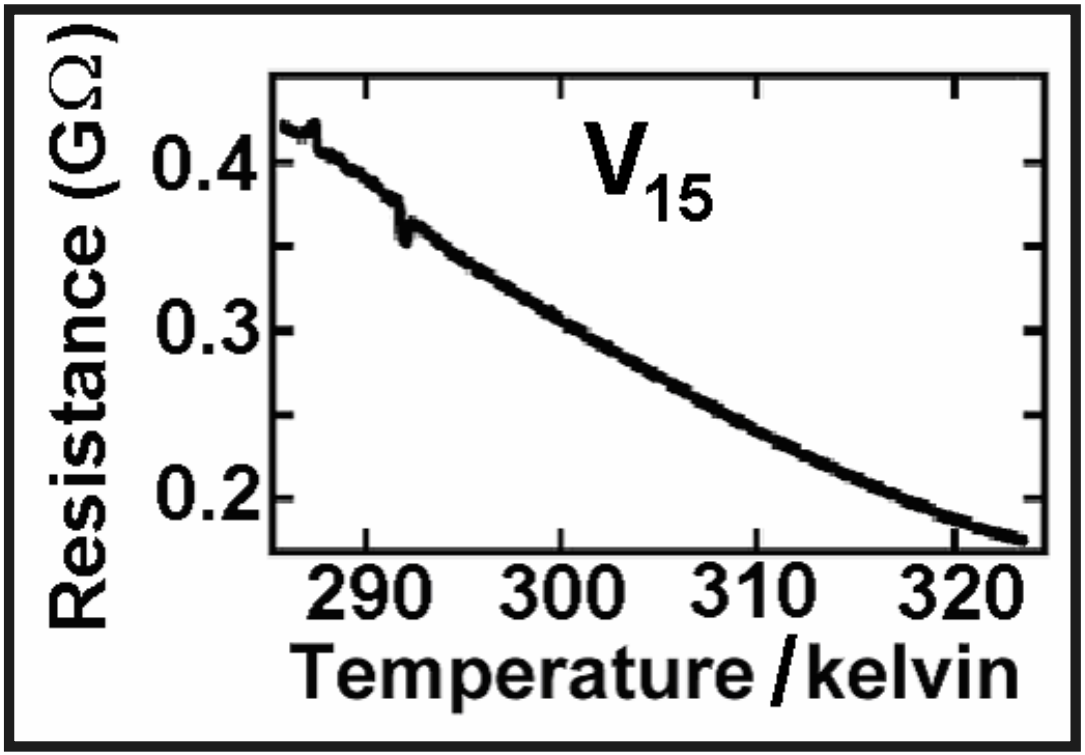

- PMMA
- Temperature dependence of the loss component of the complex dielectric constant
- $\varepsilon'' = \sigma / \omega$
- $\sigma = 1/\rho$
- Activated, Ohmic behavior above 285 K

Transport Gap

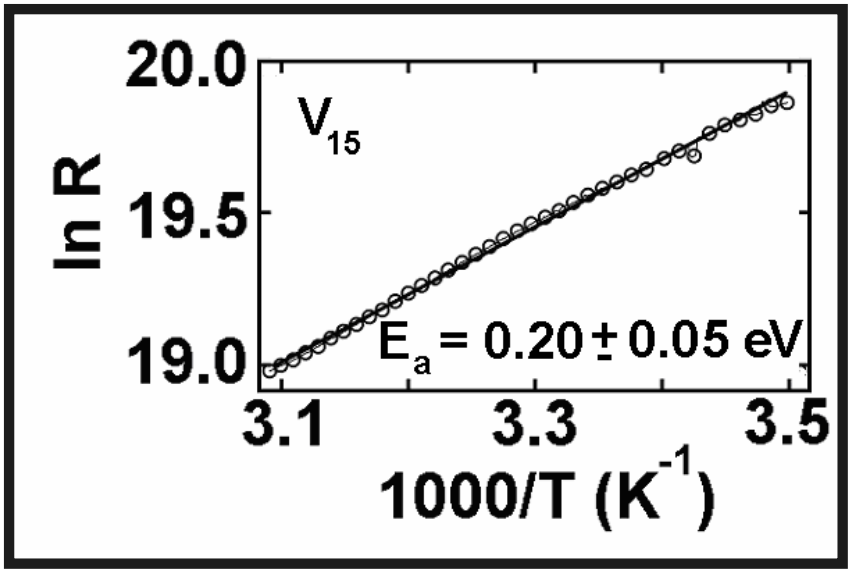

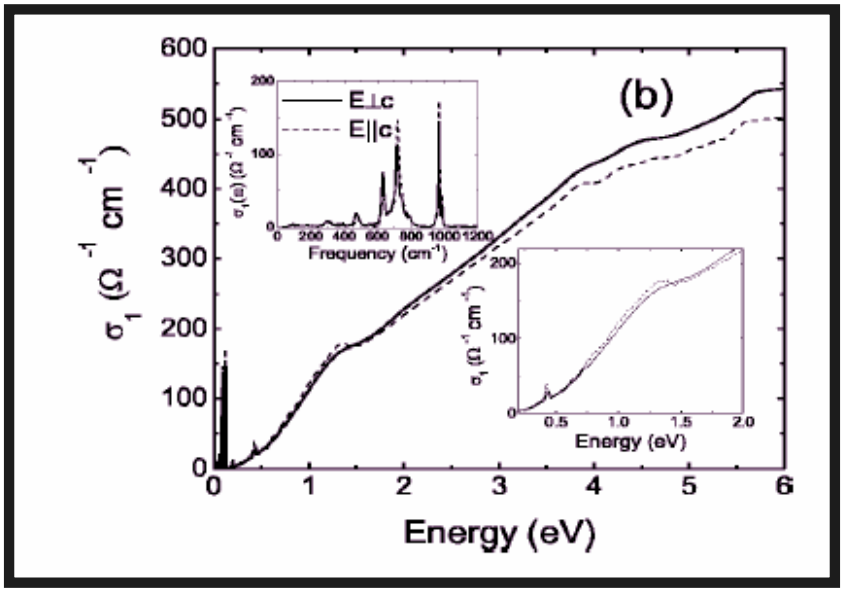

- $R(T) \sim \exp(E_a/kT)$
- $E_a \approx \frac{1}{2} E_g$
- $E_a = 0.2 \pm 0.05$ eV
- $E_g \approx 0.5$ eV

J. Choi *et al., Phys. Rev. B* **68,** 064412 (2003).

Summary

- V_{15} shows two independent dielectric relaxation modes
- V_{15} has a temperature-independent static dielectric constant of 6 ± 1
- The α mode is facilitated by intramolecular vibrations and has an activation energy of E_a = 0.22 ± 0.05 eV

Band Gap Summary

	Conductivity	Optical	Theoretical
Mn_{12}-Ac	0.74 ± 0.1 eV [a]	1.08 eV [b]	0.45 eV [c]
		1.75 eV [d]	2.08 eV [e]
			0.85 eV [f]
			1.10 eV [g]
Fe_8Br_8	1.46 ± 0.2 eV [a]		0.9 eV [h]
			0.9 eV [i]
V_{12}	0.48 ± 0.05 eV	1.2 eV	
V_{15}	0.2 ± 0.05 eV	0.5 eV	

[a]Present work, assuming $E_g = 2E_a$.
[b]Oppenheimer *et al.* (Ref. 44), minority spin cluster.
[c]Pederson *et al.* (Ref. 45), minority spin cluster.
[d]Oppenheimer *et al.* (Ref. 44), majority spin cluster.
[e]Pederson *et al.* (Ref. 45), majority spin cluster.
[f]Zeng *et al.* (Ref. 46), minority spin cluster.
[g]Zeng *et al.* (Ref. 46), majority spin cluster.
[h]Pederson *et al.* (Ref. 50), minority spin cluster.
[i]Pederson *et al.* (Ref. 50), majority spin cluster.

Conclusions

- All of these novel materials have semiconductor behavior
- Proposed mechanism for semiconductivity involves intermolecular electron hoping

Future Work

- Increase of conductivity via doping or other methods.
- Comparison with conduction from single molecules.
- Angular variation of conductivity.

Recent Studies: NMR

- Single Crystal vs. Powder NMR
- Angular dependence and field dependence studies.
- Need broad field and frequency sweeping capabilities.
- Possible because of locally developed instrumentation at the National High Magnetic Field Laboratory.

Why NMR?

- Very sensitive to electrons and local magnetic environment
- Allows check of theoretical spin alignment models
- Compliments neutron scattering data
- Distinguishes between different isomers

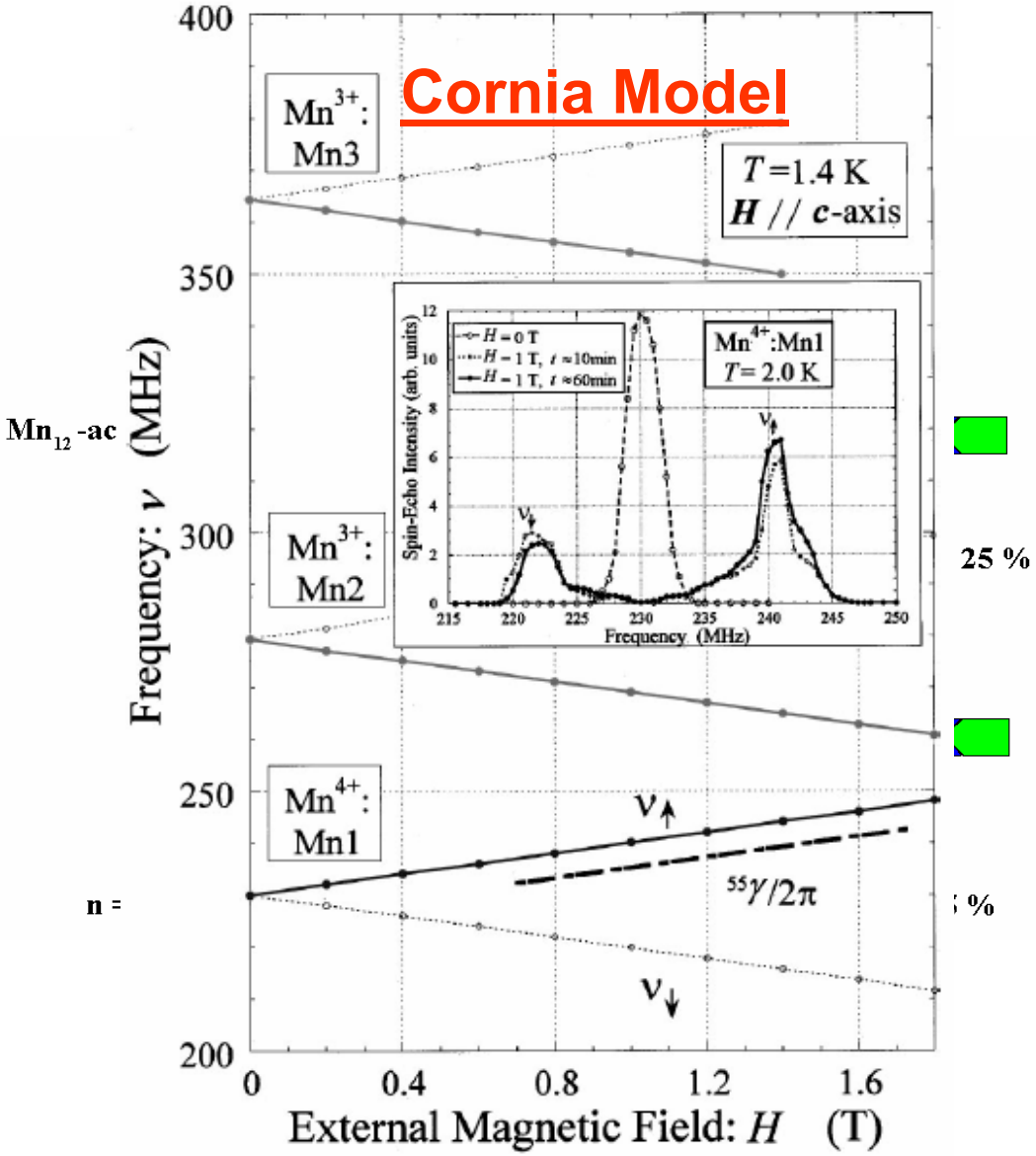

NMR Difficulties

- Strongly paramagnetic systems
- Small sample size (mm sized crystals)
- Spectral width up to ~30MHz
- Short T_{1e} (nanoseconds)
- Low T_b (Below 3K)
- No commercial instruments

Aligned Powder Sample Preparation

- Sample preparation:
  - Crush sample
  - Mix with Stycast Epoxy 1266
  - Place in a tape form
  - Set in field of 8.5 T overnight
- Possible problems:
  - Pressure and heat from crushing
  - Loss of solvent molecules

Single Crystal Sample Preparation

- Single crystals
  - Removed from mother liquor
  - Immediately covered in 5 minute epoxy
  - Cut shape out of epoxy
  - Wrap in Teflon tape

Hyperfine and Quadrupole

- Hyperfine field (mainly Fermi contact) respor
- Quadrupole interaction split energy levels fur

$$E_{\pm 5/2} = \left(\mp 5/2\right)A + B\left[\frac{18.75 - 8.75}{40}\right]$$

$$E_{\quad} = \left(\mp 5/\right)A + 0.25B$$

$$\mathcal{H} = I \cdot A \cdot S + \mathcal{H}_Q$$

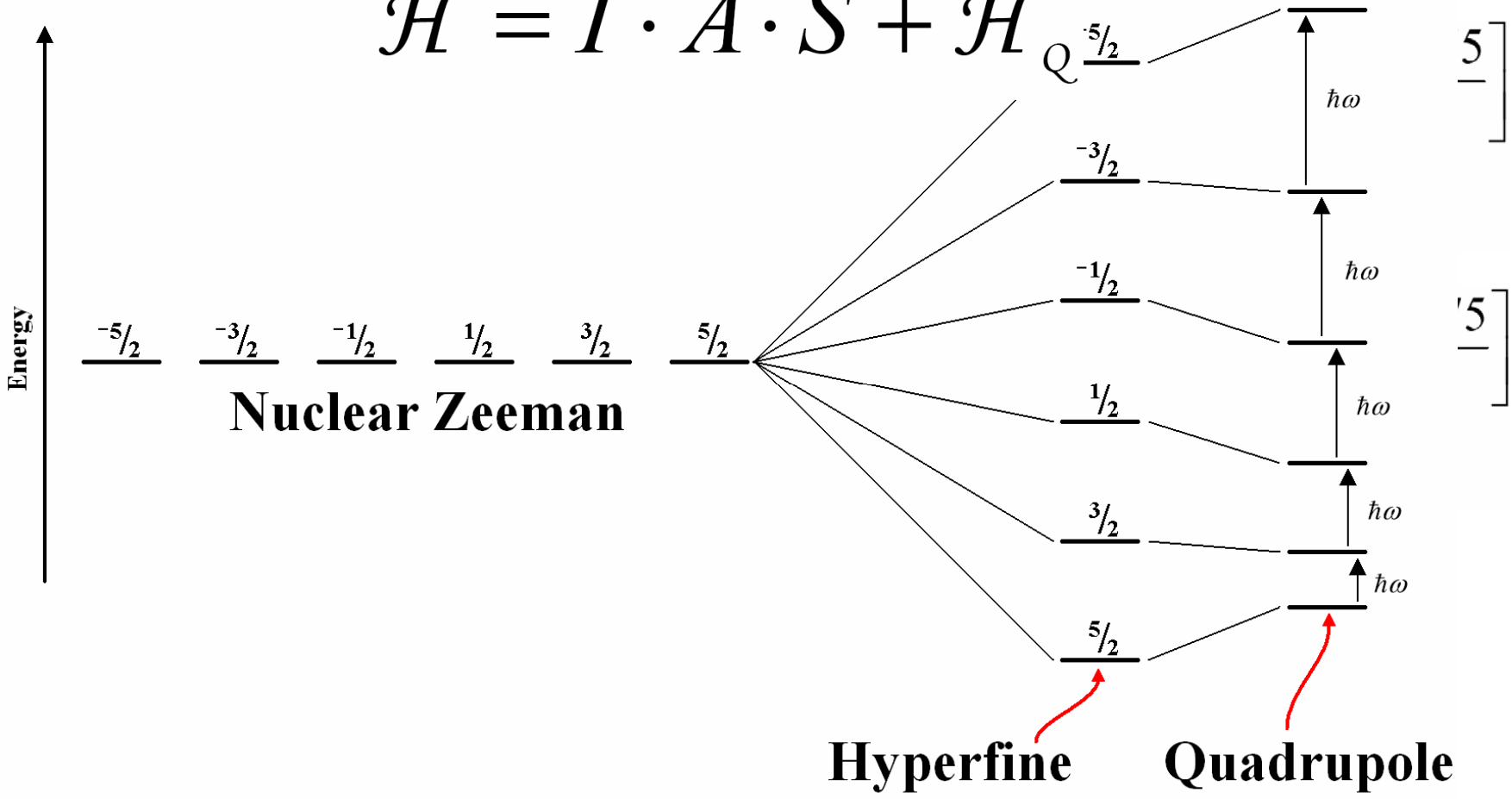

SMM investigated

- Mn_{12}-BrAc

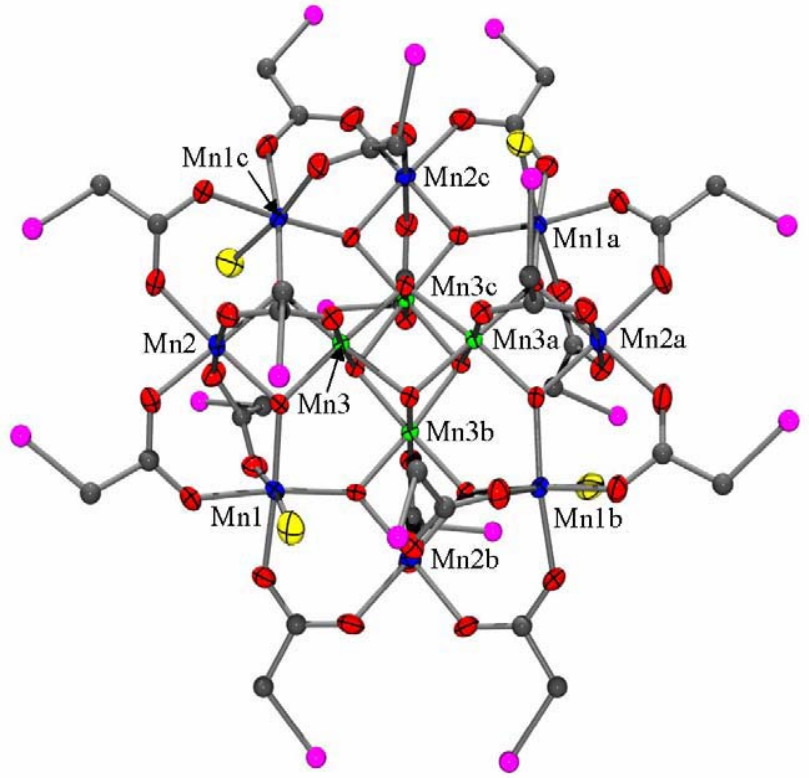

- Mn_{12}-Ac

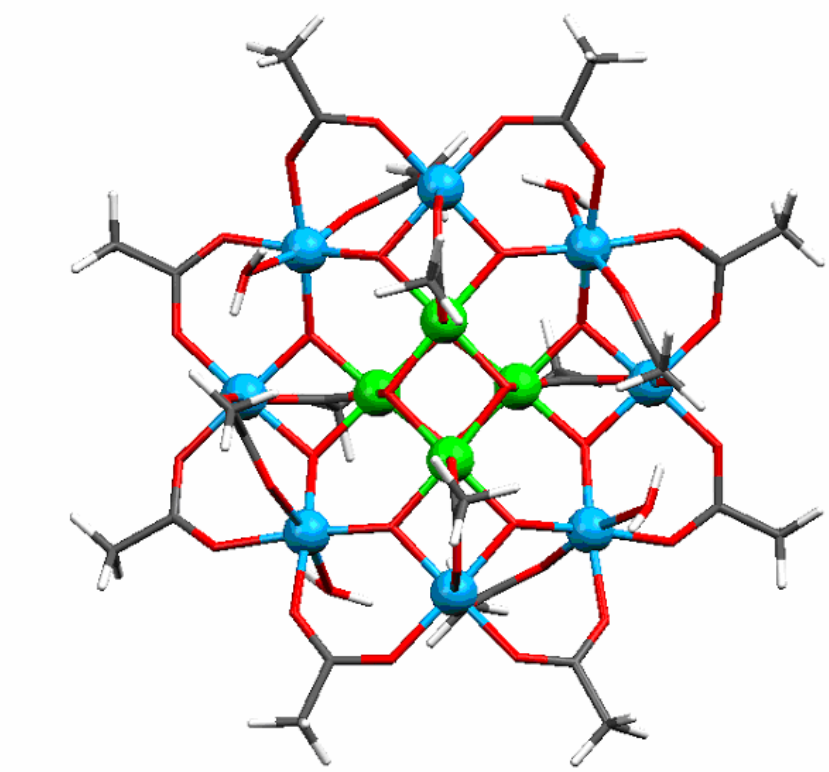

$[Mn_{12}O_{12}(O_2CCH_2Br)_{16}(H_2O)_4]\cdot 4CH_2Cl_2$

(Mn_{12}-BrAc)

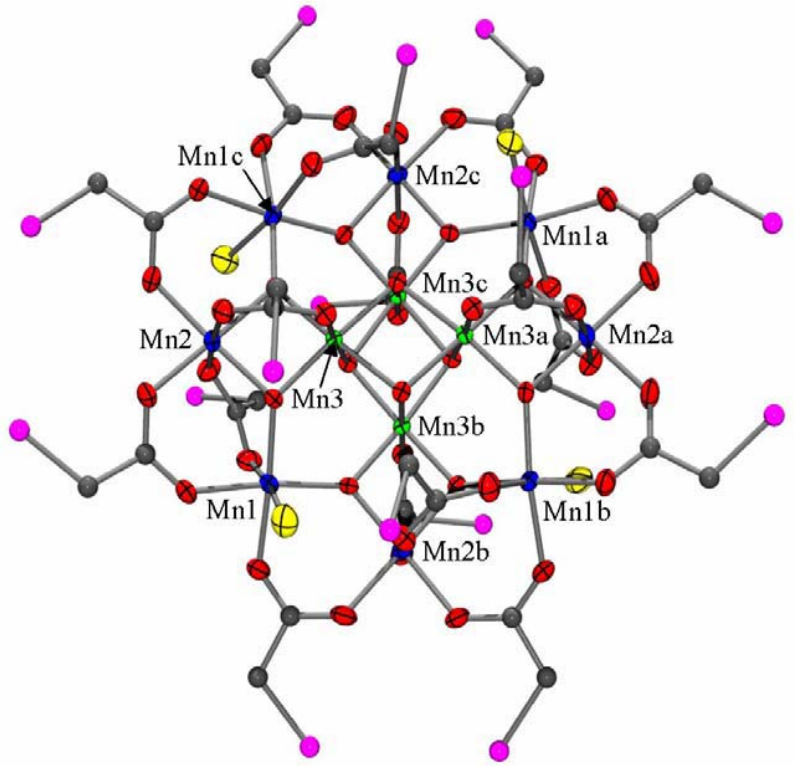

- $I4_1/a$ space group
- S = 10
- D = -0.456 cm^{-1}
- B_4^0 = -2.0 x 10^{-5} cm^{-1}
- Closest Mn-Mn distance is 6.07Å
- 4 CH_2Cl_2 solvent molecules

Aligned Powder Mn_{12}-BrAc

- Aligned powder samples were created as described earlier
  - No quadrupolar splitting noticed
  - Peaks look symmetric
- Temperature ~1.79K

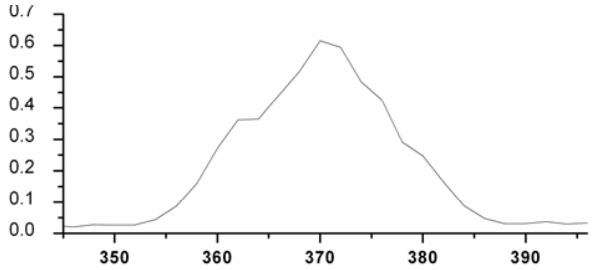

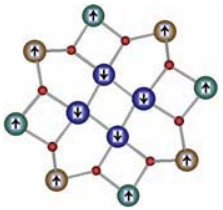

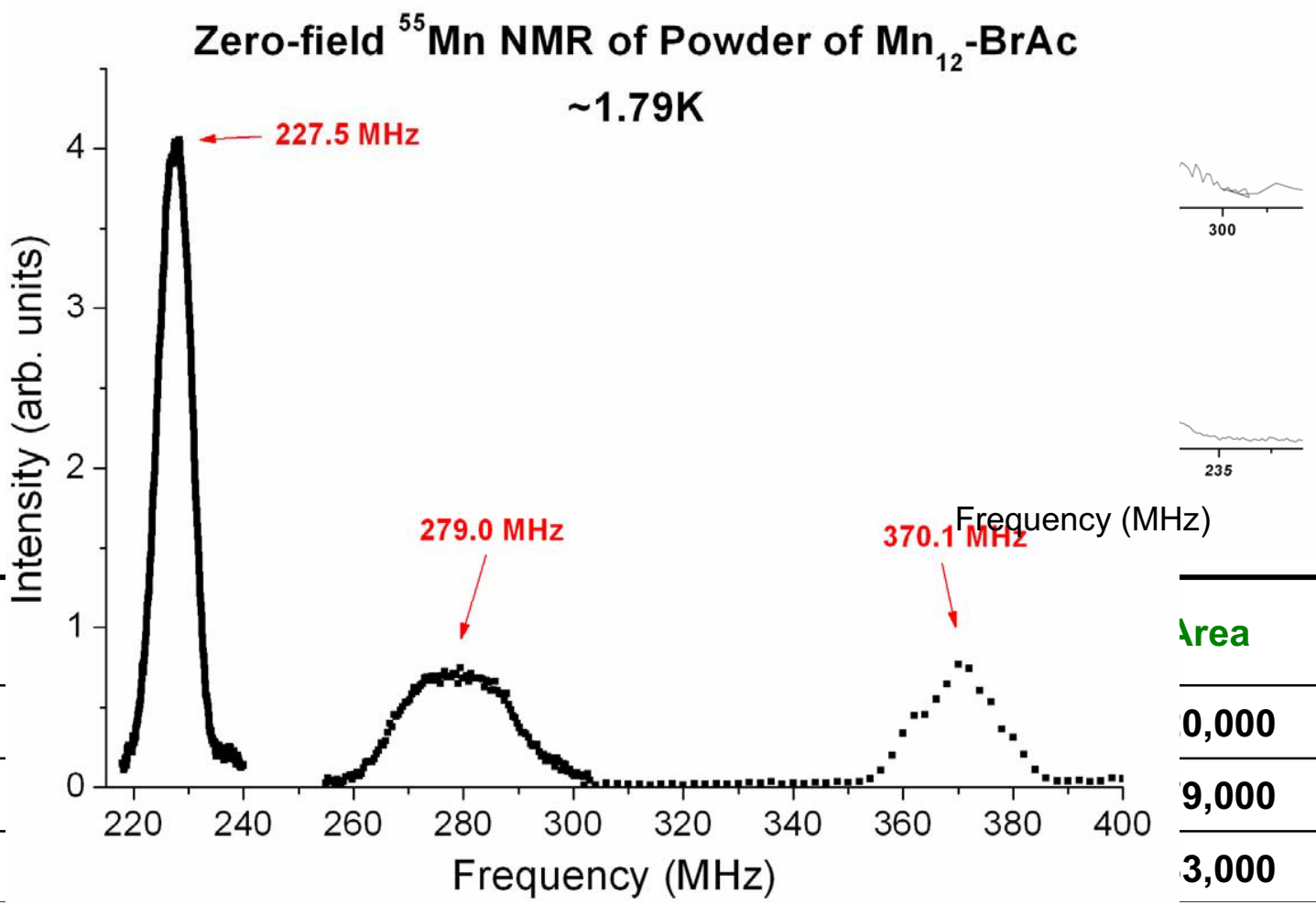

	Area
Peak 1 (Mn^{4+})	0,000
Peak 2 (Mn^{3+})	9,000
Peak 3 (Mn^{3+})	3,000

Single Crystal Mn_{12}-BrAc

- Single crystal was prepared as described earlier
- Temperature ~1.3K
- Single crystal information can be obtained from 2nd and 3rd peaks
- First peak is not split

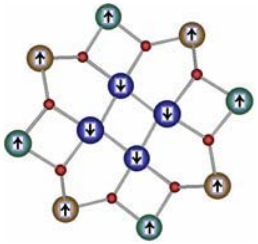

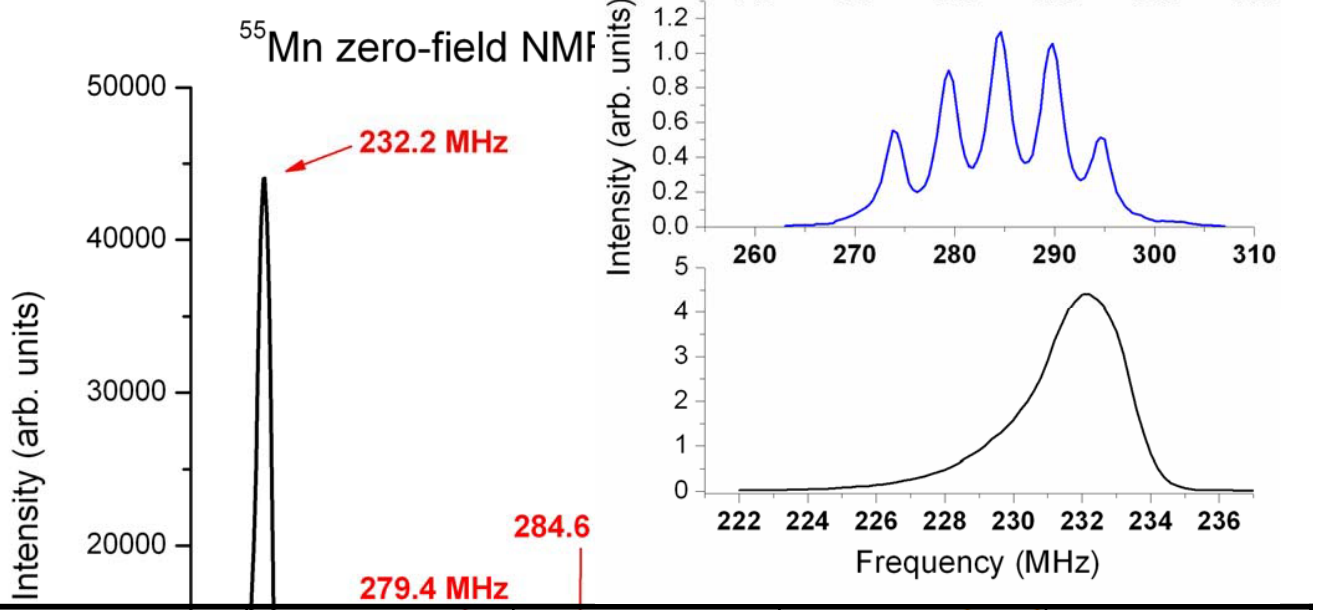

	Central Frequency (MHz)	Internal Field (Tesla)	Full Width and Half Max (MHz)	Angle from c-axis (degrees)	e^2qQ (MHz)	Area
Peak 1 (Mn^{4+})	232.2	22.01	2.96	0	0	152,000
Peak 2 (Mn^{3+})	284.6	26.98	2.99	7.9	35.33	136,000
Peak 3 (Mn^{3+})	354.1	33.56	13.76	34.0	41.43	344,000

Single Crystal vs. Powder Mn_{12}-BrAc

- Powder does not represent a statistical average of crystal
- Peaks shifted up to ~16 MHz
- Loss of Quadrupolar information
- Change most likely a result of powdering process (heat and pressure)

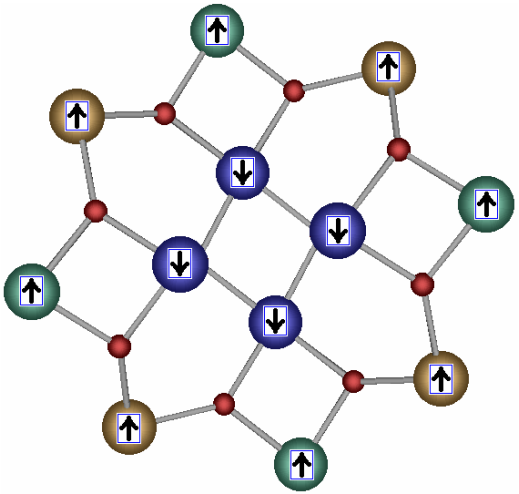

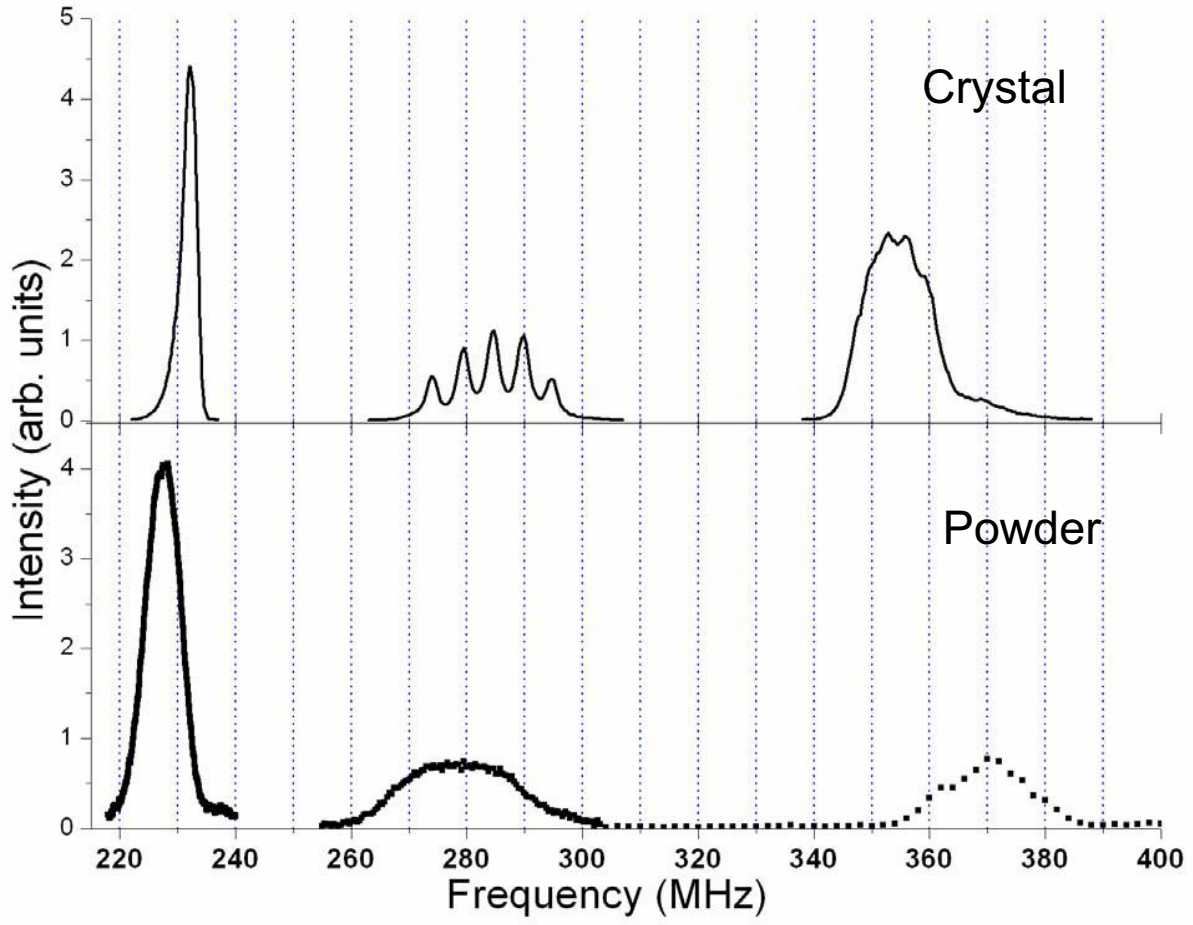

Field Studies of Mn_{12}-BrAc

- Zero-field cooled experiment
- Splitting as field is applied perpendicular to c-axis may be due to crystal mis-alignment

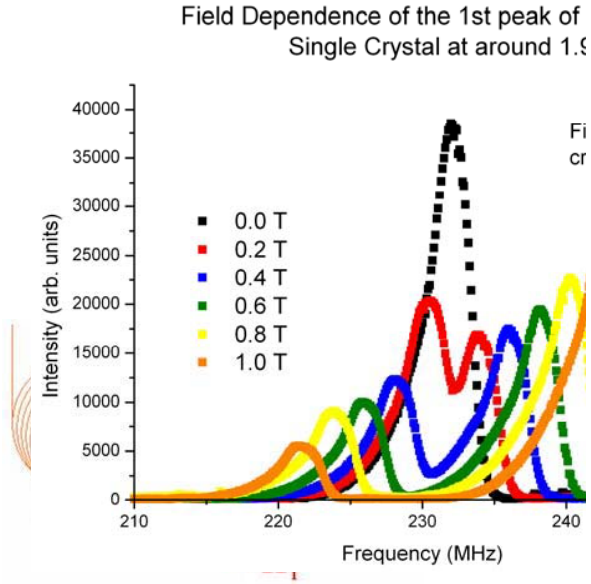

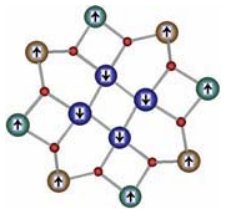

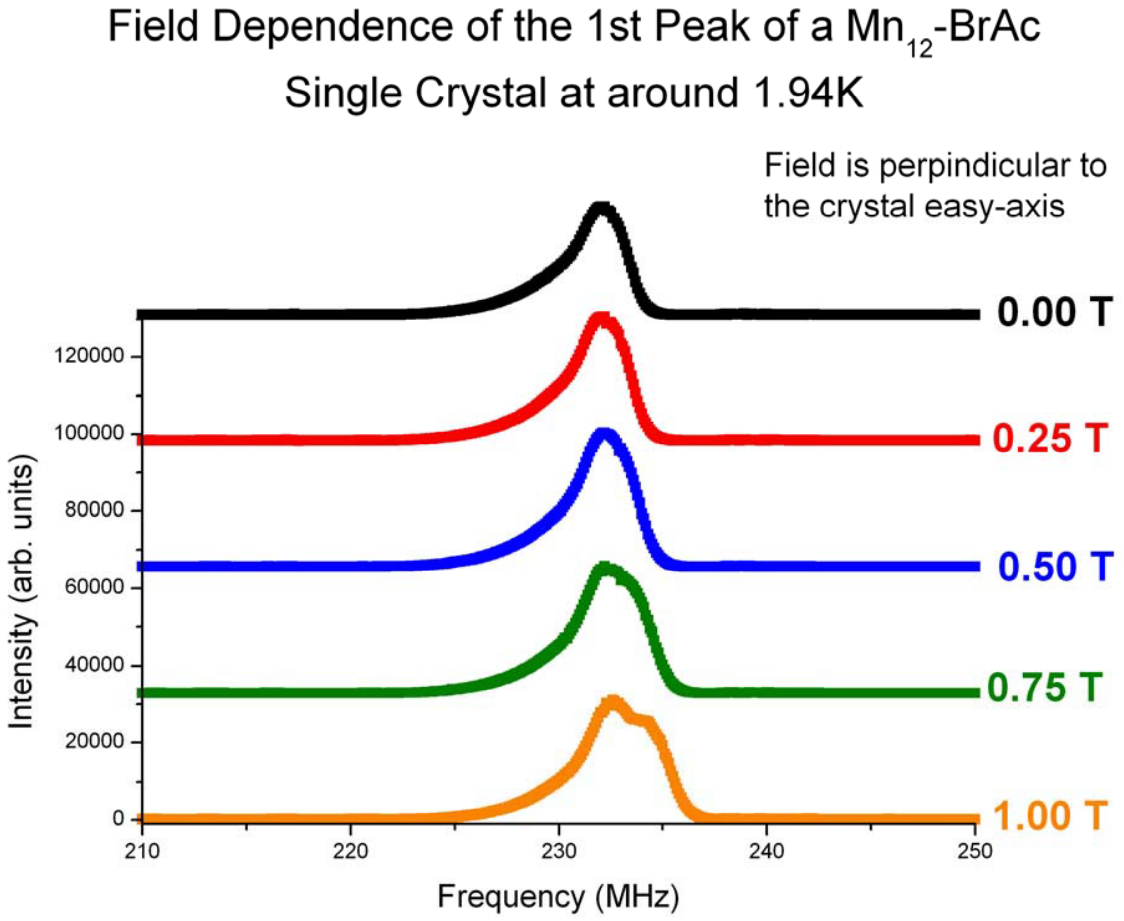

Angular Dependence Mn_{12}-BrAc: ab plane

- Crystal was prepared as previously discussed
- Experiment was done by cooling in a field of 5T
- Hyperfine fields on the ions have some component in the ab plane
- Typeak was examined because goniometer probe is set up for low frequencies

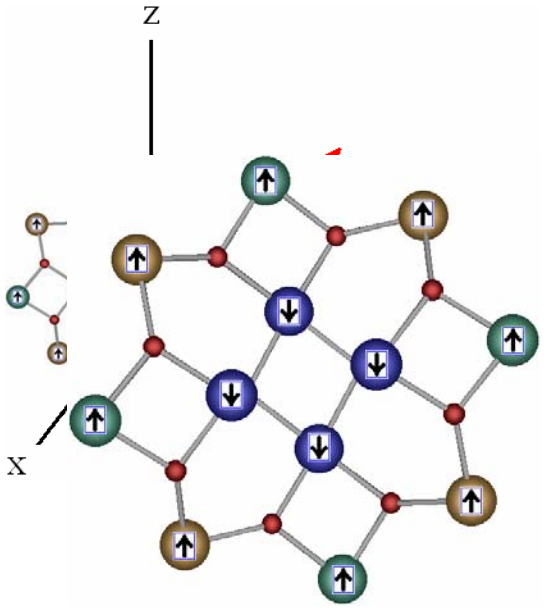

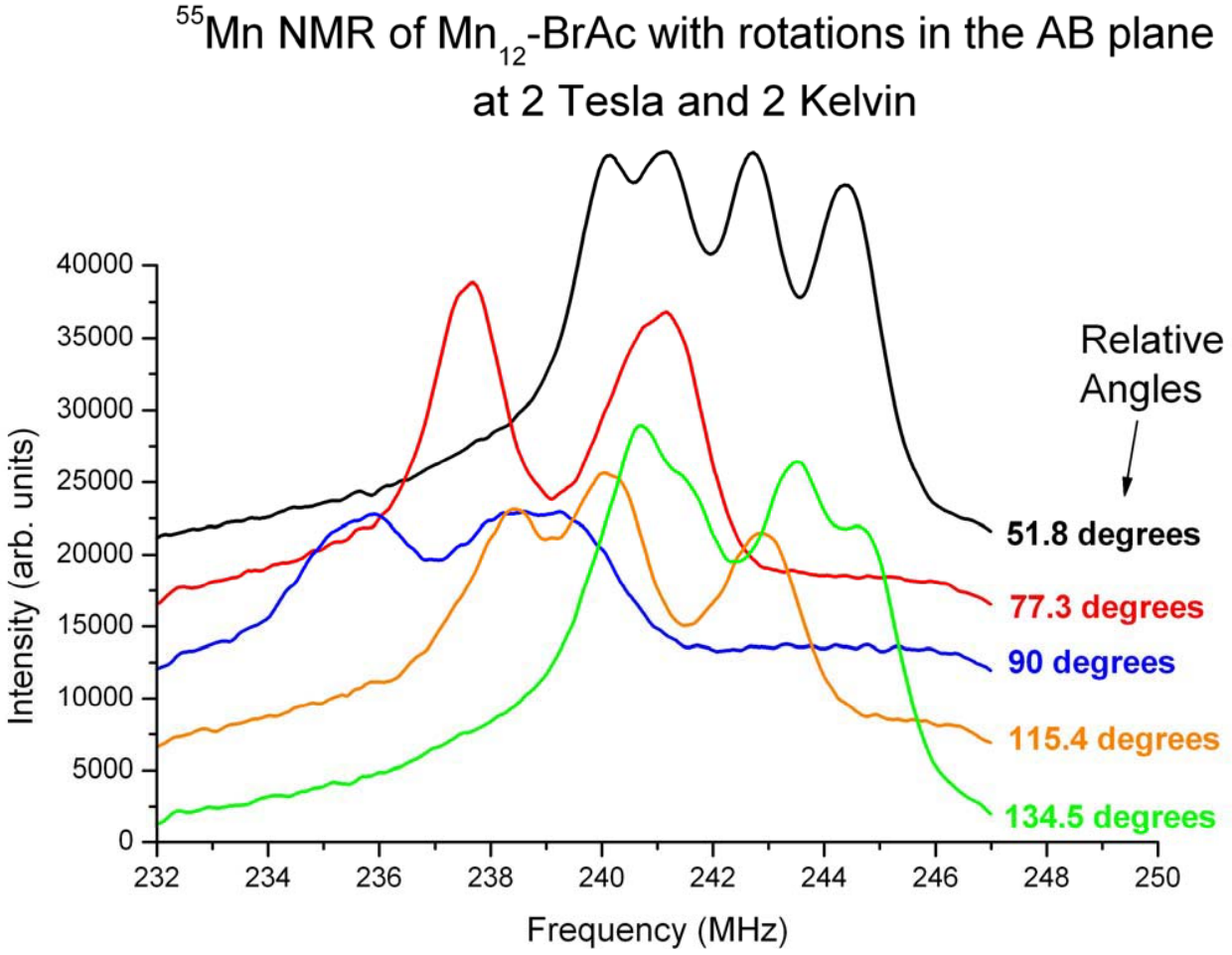

$[Mn_{12}O_{12}(CH_3COO)_{16}(H_2O)_4]\cdot 2CH_3COOH\cdot 4H_2O$

(Mn_{12}-Ac)

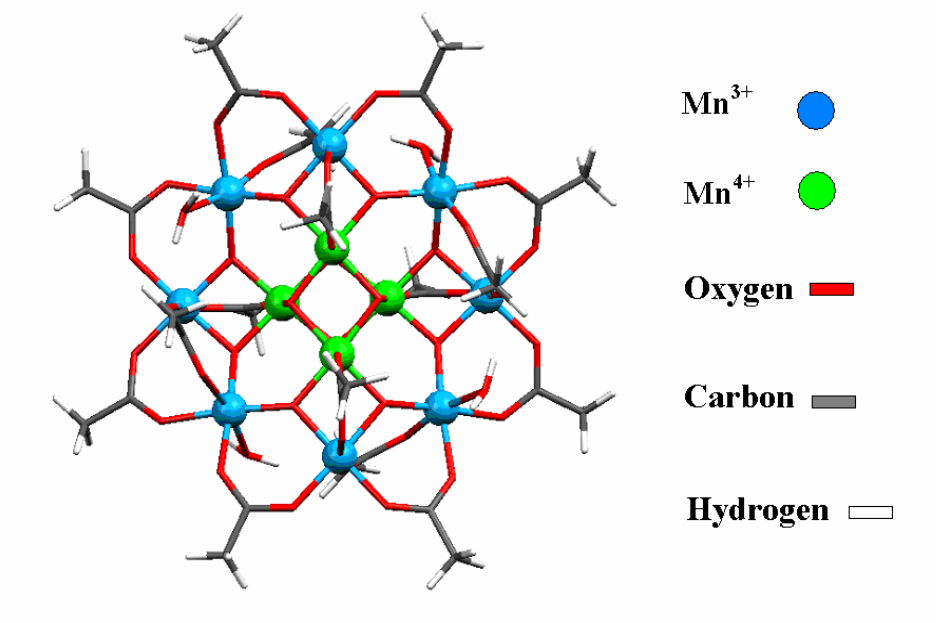

- I4(bar)
- S = 10
- D = -0.39 cm^{-1}
- B_4^0 = -7.7 x 10^{-4} cm^{-1}
- 2 HAc and 4 H_2O solvent molecules

T. Lis, *Acta Crysallogr. Sect. B* **36**, 2042 (1980).

Aligned Powder Mn_{12}-Ac

- Japanese group states that each peak has quadrupole splitting
- Can count at least 6 peaks inside of first peak
- More than 5 peaks make up the second peak

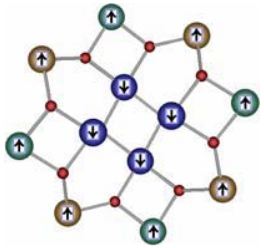

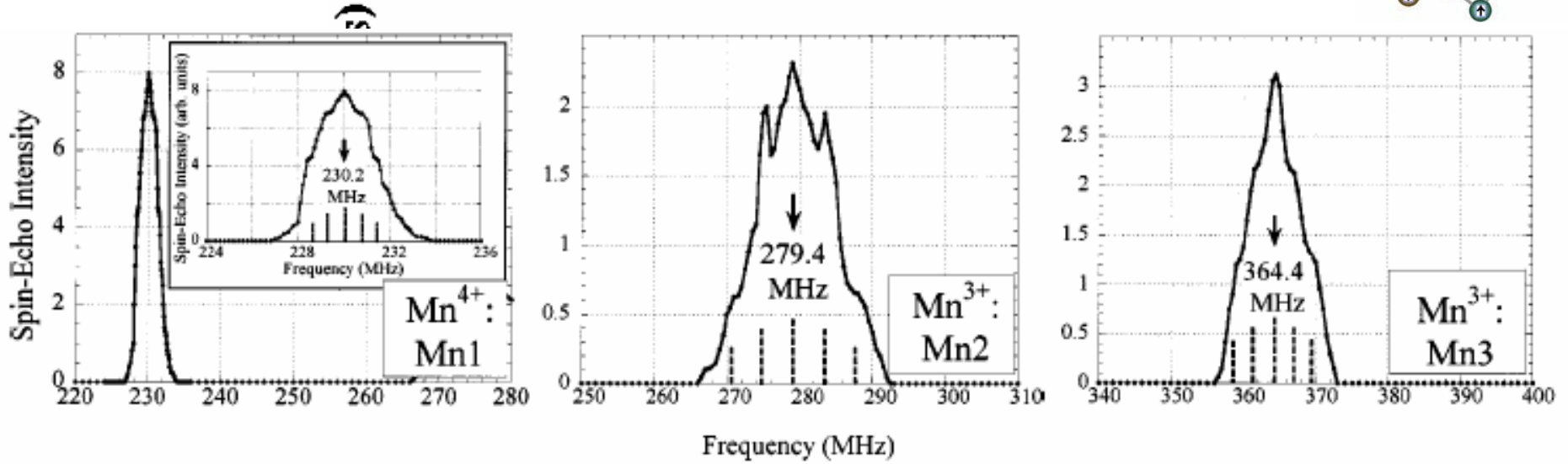

	Central Frequency (MHz)	Internal Field (Tesla)
Peak 1 (Mn^{4+})	230.2	21.82
Peak 2 (Mn^{3+})	279.4	26.48
Peak 3 (Mn^{3+})	364.4	34.54

Kubo, T. et al.; Phys. Rev. B 65, 2224425 2002

Cornia et al.

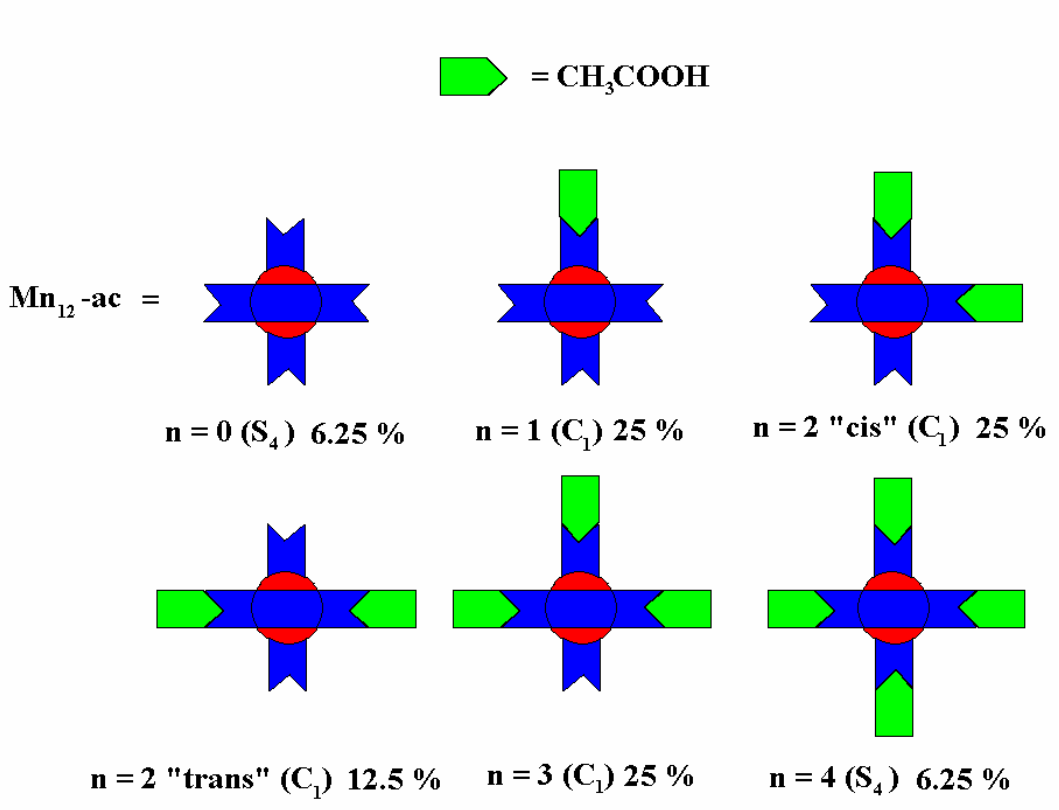

- Only two combinations have S_4 symmetry.
- Lower than S_4 gives rise to transverse field effects

A. Cornia *et al.*, *Phys. Rev. Lett.* **89**, 257201-1-4 (2002).

Single Crystal Mn_{12}-Ac

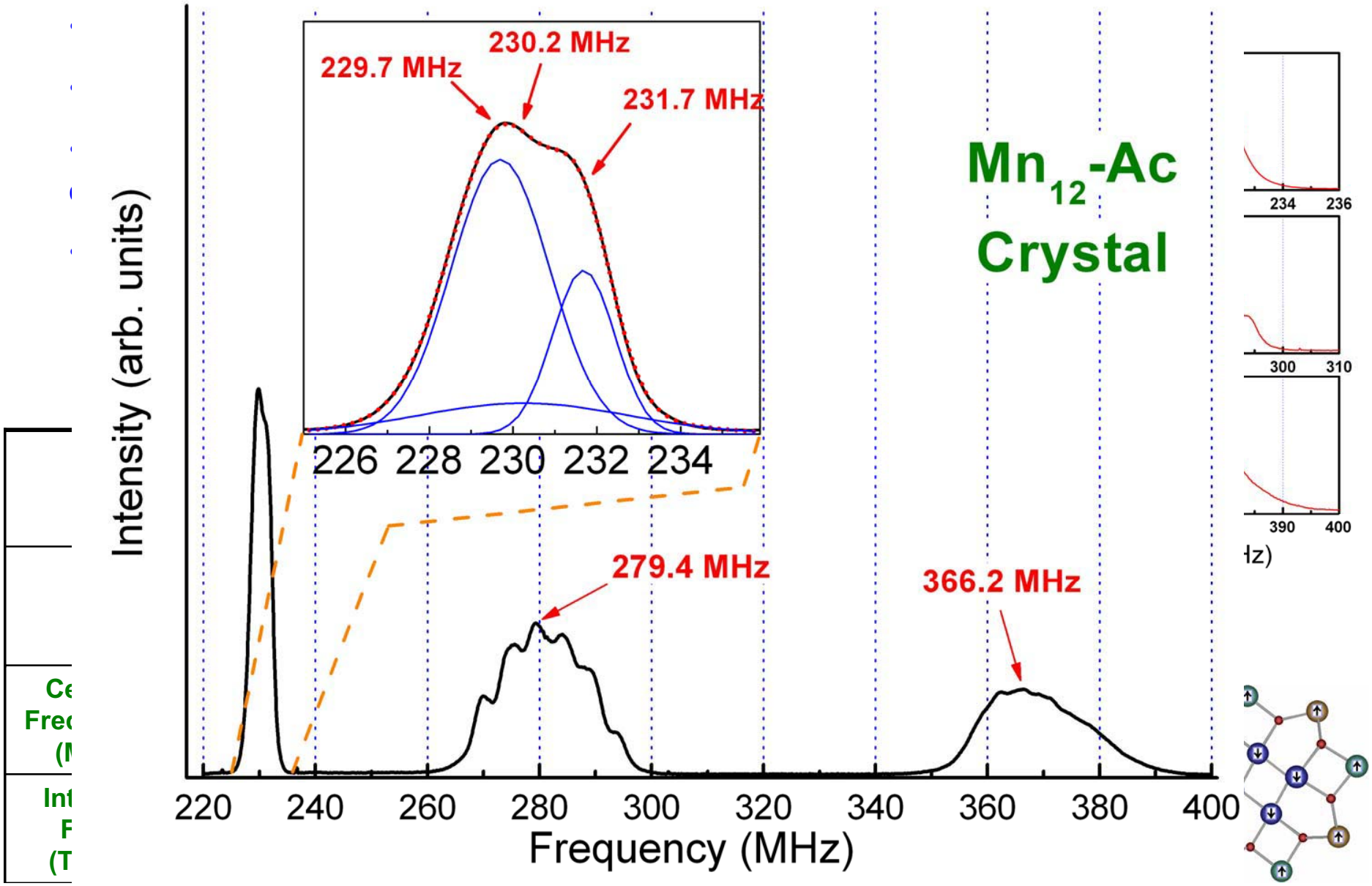

Single Crystal vs. Aligned Powder of Mn_{12}-Ac

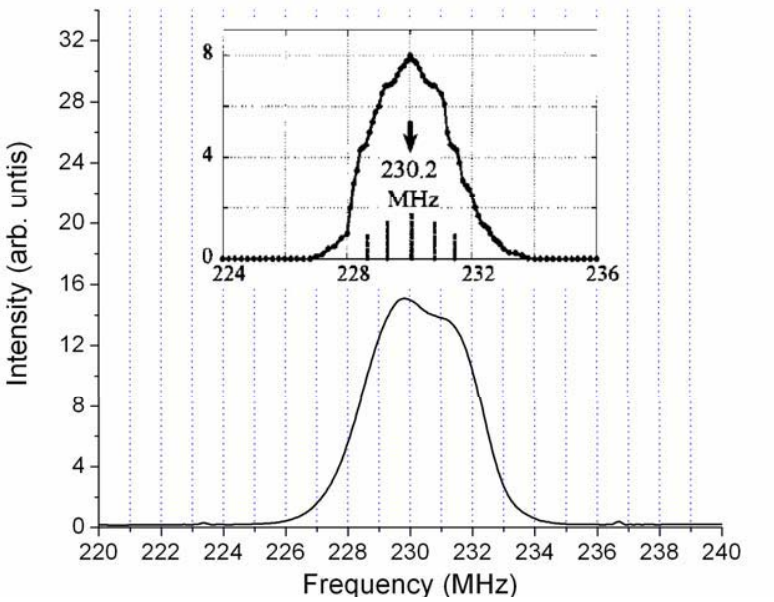

- No sign of quadrupolar splitting in first peak
- Narrower peaks from aligned powder most likely due to loss of isomers by crushing sample
- Powdering sample changes local environment at the nucleus

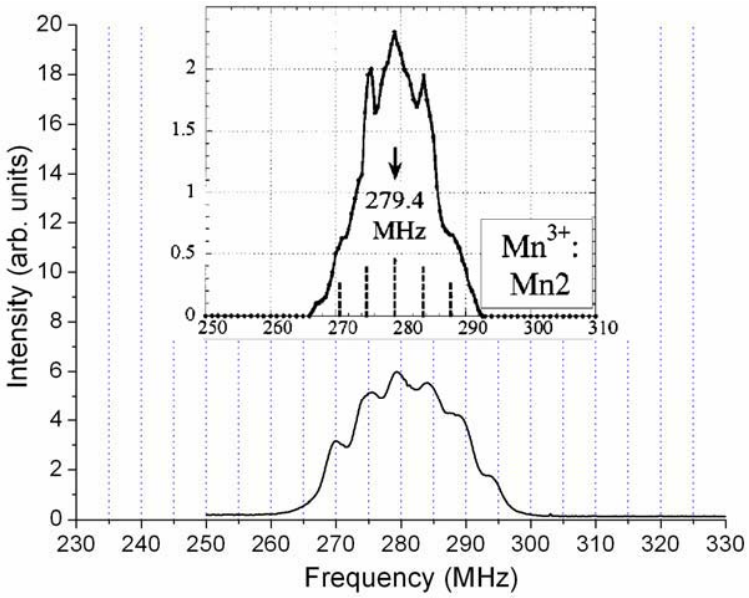

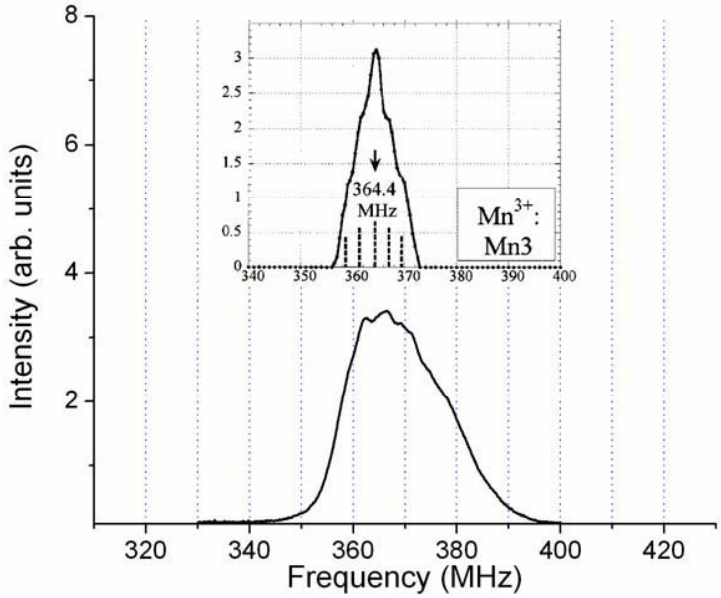

Conclusion

- NMR resolution from single crystals is much better than that obtained from aligned powders.
- Powdering of crystals causes sample defects in the lattice due to loss of solvated molecules.
- Angular dependence studies show the hyperfine interaction on the Mn^{4+} ions have an anisotropic component accounting for ~2% of the internal field. Not detectable by aligned powder NMR.
- NMR is a quicker, inexpensive technique to compliment neutron scattering for determining oxidation state and spin orientation of individual metal centers.
- NMR also compliments high field EPR data since EPR yields global (molecular) spin behavior, not that of individual ions in a complex.

Acknowledgements

- Dr. Christou
- Andrew Harter and Dr. Achey
- Dr. Reyes and Dr. Kuhns
- Funding by NSF/NIRT-DMR Grant No. 0103290